Quantumness and its hierarchies in \mathcal{PT} -symmetric down-conversion models

Jan Peřina, Jr. 0*

Joint Laboratory of Optics, Faculty of Science, Palacký University, 17. listopadu 12, 771 46 Olomouc, Czech Republic and Institute of Physics of the Academy of Sciences of the Czech Republic, Joint Laboratory of Optics of Palacký University and Institute of Physics AS CR, 17. listopadu 50a, Olomouc 772 07, Czech Republic

Karol Bartkiewicz, Grzegorz Chimczak, Anna Kowalewska-Kudlaszyk, and Adam Miranowicz. Institute of Spintronics and Quantum Information, Faculty of Physics and Astronomy,

Adam Mickiewicz University, 61-614 Poznań, Poland

Joanna K. Kalaga and Wiesław Leoński Quantum Optics and Engineering Division, Faculty of Physics and Astronomy, University of Zielona Góra, Prof. Z. Szafrana 4a, 65-516 Zielona Góra, Poland

(Received 14 May 2025; accepted 23 September 2025; published 29 October 2025)

We investigate the hierarchy of quantum correlations in a quadratic bosonic parity-time-symmetric system (PTSS) featuring distinct dissipation and amplification channels. The hierarchy includes global nonclassicality, entanglement, asymmetric quantum steering, and Bell nonlocality. We elucidate the interplay between the system physical nonlinearity (which serves as a source of quantumness) and the specific dynamics of bosonic PTSSs, which are qualitatively influenced by their damping and amplification characteristics. Using a set of quantifiers (including local and global nonclassicality depths, negativity, steering parameters, and the Bell parameter) we demonstrate that the standard PTSS typically exhibits weaker quantumness than its counterparts affected solely by damping or solely by amplification. Both the maximum values attained by these quantifiers and the speed and duration of their generation are generally lower in the standard PTSS. A comparative analysis of three two-mode PTSSs (standard, passive, and active) with identical eigenvectors and real parts of eigenfrequencies, but differing in their damping and amplification strengths, reveals the crucial role of quantum fluctuations associated with gain and loss. Among them, the passive PTSS yields the most strongly nonclassical states. Nevertheless, under suitable conditions, the standard PTSS can also generate highly nonclassical states. The supremacy of the passive PTSS is further supported by its fundamental advantages in practical realizations.

DOI: 10.1103/9vty-ctf7

I. INTRODUCTION

Since the seminal works on parity-time-symmetric systems (PTSSs) by Bender *et al.* [1,2], non-Hermitian Hamiltonians with real eigenvalues have attracted considerable attention in the physics community [3]. This interest stems from the fact that PTSSs possess unique structures in their Hilbert (or Liouville) spaces, which exhibit degeneracies, both in eigenvalues and eigenvectors, at specific parameter values known as exceptional points (EPs). These degeneracies give rise to a variety of intriguing physical phenomena (for details, see Ref. [4,5]). Systems operating at or near EPs can be harnessed for a range of applications, including enhanced sensing [6–8], enhanced nonlinear interactions [9–12], unidirectional light propagation [13,14], and even invisibility cloaking [15,16].

Published by the American Physical Society under the terms of the Creative Commons Attribution 4.0 International license. Further distribution of this work must maintain attribution to the author(s) and the published article's title, journal citation, and DOI.

Interesting behaviors of nonlinear optical systems have also been studied under PTSS conditions, i.e., when damping and amplification are balanced. It has been shown that highly nonclassical states can be generated in such systems under suitable conditions [9–12], despite the unavoidable noise present in quantum systems involving damping and/or amplification [17]. This raises an important question: to what extent does the specific dynamics in the Hilbert space of bosonic PTSSs influence the ability of system physical nonlinearities (though analyzed in many cases in their linearized versions) to generate quantumness [18–21]? The system's dynamics affect the rate at which different forms of quantumness emerge, the maximal values attained by various quantifiers, and their asymptotic limits. A fundamental problem thus arises: Can the specific dynamics in the Hilbert space of a PTSS enhance the ability of physical nonlinearities to generate diverse forms of nonclassical states?

In this paper, we address in detail this complex issue by the extended numerical analysis of different versions of two-mode bosonic \mathcal{PT} -symmetric system with parametric down-conversion that covers the entire system's parameter space and includes all common forms of quantumness (system nonclassicality, entanglement, steering, and the Bell

^{*}Contact author: jan.perina.jr@upol.cz

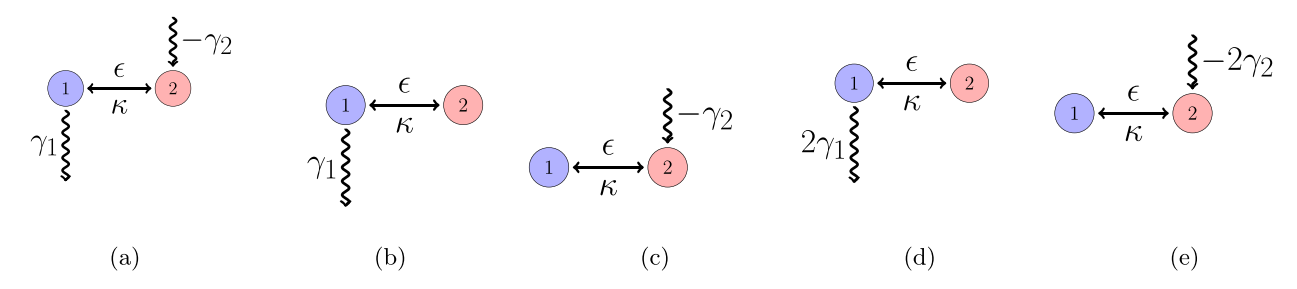


FIG. 1. Schematics of the two-mode bosonic system analyzed under different conditions: (a) standard \mathcal{PT} -symmetric system, where mode 1 is damped ($\gamma_1 > 0$) and mode 2 is amplified ($\gamma_2 < 0$); (b) system with only mode 1 damped ($\gamma_1 > 0$); (c) system with only mode 2 amplified ($\gamma_1 > 0$); (d) passive $\gamma_1 = 0$; (e) passive $\gamma_2 = 0$; (e) active $\gamma_2 = 0$; (f) active $\gamma_2 = 0$; (e) active $\gamma_2 = 0$; (e) active $\gamma_2 = 0$; (e) active $\gamma_2 = 0$; (f) active $\gamma_2 = 0$; (g) active $\gamma_2 = 0$; (e) active $\gamma_2 = 0$; (f) active $\gamma_2 = 0$; (f) active $\gamma_2 = 0$; (g) active $\gamma_2 = 0$; (f) acti

nonlocality). The emergence of quantumness is discussed as competition between the system's coherent dynamics and detrimental influence of the reservoir fluctuating forces. The obtained complete numerical analysis allows us to draw even several general conclusions. Whereas the coherent dynamics does not allow to fully compensate for the influence of the reservoir forces for the most of the parameters in the standard PTSS, it leads to the generation of the states with high levels of quantumness in the passive PTSS.

The paper is structured as follows. In Sec. II we discuss the general behavior of bosonic \mathcal{PT} -symmetric systems whose properties emerge in the competition between their coherent evolution and the influence of the noise inevitably accompanying damping and amplification present in the system. In Sec. III, the considered PTSS is introduced, its solution is found, and statistical properties of its modes are described considering Gaussian fields. Nonclassicality depths, negativity, steering parameter and the Bell parameter are introduced and determined for the Gaussian fields in Sec. IV. The role of standard $\mathcal{P}\mathcal{T}$ symmetry in nonclassical-state generation is elucidated in Sec. V using the comparison with the systems influenced only either by damping or amplification. In Sec. VI, relying on similarity of coherent dynamics in the standard PTSS, passive PTSS with doubled damping, and active PTSS system with doubled amplification [see the scheme in Figs. 1(a), 1(d), and 1(e)], the role of reservoir fluctuations accompanying damping and amplification in nonclassicalstate generation is elucidated. Section VII is devoted to the comparison of the PTSSs ability to generate different forms of quantumness and quantum correlations. Time and speed aspects of the nonclassical-state generation are addressed in Sec. VIII. Conclusions are drawn in Sec. IX.

II. COMPETING EFFECTS OF COHERENT DYNAMICS AND RESERVOIR NOISE IN QUANTUM \mathcal{PT} -SYMMETRIC SYSTEMS

When we look back at the history, PTSSs were extensively studied within the framework of classical physics (see Refs. [22,23] and Refs. [4,24–27]), particularly in optics, where their specific coherent dynamics proved especially beneficial. A hallmark of PTSSs is the simplification of system dynamics at EPs, often accompanied by the enhancement of certain system properties. The extension of these concepts to quantum

optical bosonic systems, via the use of Glauber coherent states and the Glauber-Sudarshan *P* representation of the statistical operator [28,29], appeared straightforward. The idea of employing PTSSs endowed with some form of physical nonlinearity to generate various nonclassical and entangled states promised significant and attractive outcomes. Indeed, a range of nonlinear PTSSs have been used to produce nonclassical states with unusual properties [9–12].

However, a critical problem was identified: the presence of chaotic fluctuating forces, which, according to both the fluctuation-dissipation and analogous amplification-fluctuation theorems, inevitably accompany damping and amplification. Due to their chaotic nature, these forces tend to degrade all forms of system quantumness [17]. As a result, two competing effects come into play in PTSSs with respect to the generation of quantumness: while the coherent \mathcal{PT} -symmetric dynamics tends to support and enhance quantumness, the accompanying chaotic fluctuations tend to suppress it [30]. This raises a fundamental question: Can the coherent \mathcal{PT} -symmetric dynamics fully compensate for the detrimental effects of the fluctuating forces, or even enhance the system's quantumness despite their presence?

While it is difficult, if not impossible, to answer this question in full generality, valuable physical insight can be gained by analyzing specific, well-defined models. One of the simplest models that satisfies the necessary criteria involves two interacting bosonic modes, mutually coupled through both linear and (physically) nonlinear interactions and subject to damping and amplification. An important technical advantage of this model lies in the fact that, under the physically relevant conditions, the model can be analyzed in its linearized version in which its dynamical operator equations remain linear, enabling a fully analytical treatment.

By focusing on Gaussian states, we are able to analytically determine all relevant parameters characterizing the system, including the effects of averaging over the chaotic fluctuating forces. This analytical approach makes it possible to systematically explore the entire parameter space of the model, as well as to examine its temporal evolution. The study of this evolution is supported by both numerical simulations and asymptotic (long-time) analytical formulas.

Regarding the effect of noise in our system, it originates from quantum sources, as it arises from interactions with quantum reservoirs composed of two-level atoms. These

atoms are either in the ground state (in the case of damping) or in the excited state (for amplification). The quantum state of the reservoir atoms fundamentally alters the character of the reservoir-induced noise: excited atoms can induce both spontaneous and stimulated emission in the system, whereas ground-state atoms only allow for stimulated absorption. This distinction leads to the fact that amplification-related noise is more detrimental than damping-related noise: it is simply stronger [17].

However, as already mentioned above, the generation of quantum features in the system is governed by more than just the noise level; it also strongly depends on the system's physical nonlinearity, which is determined by the product of the nonlinear coupling constant and the mode amplitudes. The coherent part of the dynamics typically leads to larger mode amplitudes, especially in the presence of amplification, which can in turn enhance the generation of quantumness. This stands in contrast to the detrimental effects introduced by noise. As a result, the system's behavior emerges from the competition between these two opposing factors: chaotic noise versus coherent physically nonlinear dynamics.

This interplay lies at the heart of our investigation and constitutes the central motivation behind it. While noise often dominates and at least partially suppresses quantum effects, there exist regions in the parameter space where coherent dynamics prevail, enabling the emergence of nonclassical behavior despite the presence of noise. This delicate balance is what makes the results fundamentally interesting and potentially attractive.

The selection of an appropriate reference system is an important issue. The hallmark features of PTSSs arise from a balance between gain and loss in the modes, and these features should be absent in any suitable reference system. Such reference configurations include systems in which only one mode is subject to damping while the other evolves freely, or vice versa, one mode is amplified while the other remains unaffected. However, detailed analysis across the full parameter space reveals that, in most cases, the \mathcal{PT} -symmetric dynamics does not offer a significant advantage in generating different forms of quantumness. This suggests that the influence of chaotic fluctuating forces is typically too strong to be compensated for by coherent \mathcal{PT} -symmetric evolution.

This naturally leads us to consider more general \mathcal{PT} -symmetric-like systems, namely, their passive and active variants [31]. In passive (active) \mathcal{PT} -symmetric systems, the modes experience unequal levels of damping (amplification). However, the eigenvalues of their corresponding dynamical matrices share a common damping (amplification) component, while the remaining parts (along with the associated eigenvectors) retain the essential characteristics of standard PTSSs. As such, aside from the global damping (or amplification) factor, the coherent dynamics remain effectively identical to those of the standard PTSS counterpart. This structural similarity is promising for the generation of quantumness, provided that the impact of chaotic fluctuations is sufficiently reduced.

Indeed, the contributions of chaotic fluctuating forces are not symmetric: those associated with damping are generally weaker than those arising from amplification. This is because amplification typically involves coupling to inverted two-level atoms, which are susceptible to spontaneous photon emission, a process that significantly enhances the destructive influence of noise. Based on this observation, we analyze a passive PTSS in which one mode is subject to double damping, while the other evolves freely. As demonstrated below, this configuration turns out to be optimal for the generation of quantumness.

Nevertheless, active PTSSs, where one mode is doubly amplified and the other evolves without gain or loss, should not be dismissed *a priori*. Despite the stronger fluctuating forces inherent to amplification, the shared amplification factor can significantly enhance the system's physical nonlinearity through its influence on the coherent \mathcal{PT} -symmetric-like dynamics. While under typical conditions the detrimental effects of noise dominate, our results reveal specific parameter regimes in which amplified coherent dynamics prevail, leading to enhanced nonclassicality, as discussed in detail below.

In the paper, we analyze a two-mode bosonic system governed by a quadratic Hamiltonian [11,12,30], the original nonlinear Hamiltonian belonging to the three-mode optical nonlinear interaction is linearized by assuming a strong undepleted pump mode (parametric approximation) [18,19]. This linearized Hamiltonian includes both linear mode coupling and nonlinear interaction arising from parametric down-conversion. Though the nonlinear interaction is effectively described by its linearized form it enables the generation of quantum states. The quadratic form of the Hamiltonian yields linear Heisenberg equations of motion, which can be solved analytically [21]. These solutions incorporate fluctuating Langevin noise operators associated with damping and amplification, providing a rigorous framework for the system's dynamical analysis.

We note that we refer to the investigated model as (physically) nonlinear because the Hamiltonian in Eq. (1) below contains the terms $a_1a_2 + a_1^{\dagger}a_2^{\dagger}$, which correspond to the two-mode squeezing interaction that belongs to the group of three-mode optical nonlinear interactions described by second-order susceptibilities $\chi^{(2)}$. These interactions are capable of generating or enhancing nonclassicality and increasing the total number of excitations during evolution, in contrast to linear optical systems characterized solely by first-order susceptibilities $\chi^{(1)}$. This fundamental distinction then underpins the definition of certain nonclassicality measures, such as potentials of quantum entanglement, steering, and Bell nonlocality [32].

The approach based on linearizing the nonlinear-system dynamics and subsequent analytical treatment allow for a detailed comparison between the standard PTSS, affected by both damping and amplification, and two related configurations involving only damping or only amplification [see Figs. 1(a) to 1(c)]. By evaluating various quantifiers of quantumness, characterizing both nonclassicality and quantum correlations, we investigate how the system's specific structure impacts the formation of nonclassical states. The analyzed quantifiers include local and global nonclassicality depths [33], negativity [34,35] as a measure of entanglement, the steering parameter [36] for asymmetric quantum steering, and the Bell (nonlocality) parameter [37] for identifying the strongest type of quantum correlations among those considered.

We note that, in our analysis, we consider the so-called *quantum exceptional points* that occur in the dynamics of open quantum systems characterized by their Liouvillians. Contrary to the usual Hamiltonian EPs, they are fully compatible with the general dynamics of open quantum systems [38–41]. We note that, rather than analyzing the system's evolution via the master equation and its associated Liouvillian, we employ a more tractable approach based on the analytical solution of the corresponding Langevin-Heisenberg equations, including their Langevin noise terms [20,42]. This method not only reveals the system's eigenfrequencies (associated with the Liouvillian spectrum, cf. [39]), but also facilitates the derivation of Gaussian-state parameters through averaging over the chaotic noise forces.

III. TWO-MODE BOSONIC SYSTEM WITH DAMPING AND AMPLIFICATION

The modes are assumed to mutually interact via the linear exchange of energy (described by linear coupling constant ϵ) and the physically nonlinear addition or subtraction of photon pairs into both modes that originates in parametric down-conversion [19] (nonlinear coupling constant κ). Damping and amplification of modes, that causes the presence of additional Langevin fluctuating operator forces representing the back-action of the reservoir, describe loss and addition of energy into the modes (for the sketch of the system analyzed under different conditions, see Fig. 1). Introducing the photon annihilation (\hat{a}_j) and creation (\hat{a}_j^{\dagger}) operators of the modes denoted as 1 and 2 together with the corresponding Langevin operator forces \hat{l}_j and \hat{l}_j^{\dagger} and system-reservoir coupling constants r_j , j=1,2, we express the appropriate system interaction Hamiltonian \hat{H} as follows [20,30,39]:

$$\hat{H} = [\epsilon \hat{a}_{1}^{\dagger} \hat{a}_{2} + \kappa \hat{a}_{1} \hat{a}_{2} + \text{H.c.}] + [r_{1} \hat{a}_{1} \hat{l}_{1}^{\dagger} + r_{2} \hat{a}_{2} \hat{l}_{2}^{\dagger} + \text{H.c.}],$$
(1)

where the symbol H.c. replaces the Hermitian conjugated terms. To allow consistent description of both damped and amplified modes, we chose the Langevin operator forces \hat{l}_j and \hat{l}_j^{\dagger} , j=1,2, as the Pauli spin-flip operators that describe the reservoir two-level atoms [43]. Invoking the second-order perturbation theory in the system-reservoir coupling constants r_1 and r_2 and eliminating the reservoir operators by replacing them by their reservoir mean values [with the two-level reservoir atoms in the ground (excited) state for damping (amplification)] we reveal the corresponding damping and amplification constants as well as the appropriate mean values of the Langevin operator forces, see Eqs. (4) and (2) below as well as detailed derivation in Refs. [20,39,42].

We note that the above approach based on the Heisenberg-Langevin operator equations with the Langevin fluctuating operator forces [20] represents an alternative to the commonly used approach based on the (generalized) master equation for a statistical operator [42,44]. The convenience of the application of these approaches differs according to the situation that includes both the structure of the model and the type of the states investigated. In our case in which we pay attention to Gaussian fields [20,45], the use of the Heisenberg-Langevin operator equations is more convenient owing to the linearity

that arises in the parametric approximation applied to the nonlinear interaction [21]. In contrast, the solution of the corresponding master equation transformed into the form of the Fokker-Planck equation [46] would involve the temporal solution for the mean-field-operator amplitudes and also statistical coefficients of the Gaussian states [see Eq. (20) below]. In the applied approach, these coefficients are derived directly from the operator solution of the Heisenberg-Langevin equations. This considerably simplifies the calculations.

In the model, we assume that mode 1 is damped (damping constant γ_1) whereas mode 2 is amplified (amplification constant $-\gamma_2$). The reservoirs responsible for damping and amplification are assumed to be described by independent quantum random Gaussian and Markovian processes with the following characteristics [43,47,48], j = 1, 2:

$$\langle \hat{l}_{j}(t) \rangle = \langle \hat{l}_{j}^{\dagger}(t) \rangle = 0,$$

$$\langle \hat{l}_{j}^{\dagger}(t)\hat{l}_{j}(t') \rangle = \tilde{l}_{j}\delta(t - t'),$$

$$\langle \hat{l}_{j}(t)\hat{l}_{j}^{\dagger}(t') \rangle = l_{j}\delta(t - t').$$
(2)

In Eq. (2), the real constants l_j and \tilde{l}_j , j = 1, 2, have to be chosen such that the commutation relations for the photon creation and annihilation operators are fulfilled. These are $[\hat{a}_j, \hat{a}_i^{\dagger}] = 1$ for j = 1, 2 and the remaining commutation relations among the operators \hat{a}_j and \hat{a}_i^{\dagger} are zero. The symbol δ stands for the Dirac function. In the case of damping in mode 1 and the reservoir two-level atoms in the ground state, we have $l_1 = 2\gamma_1$ and $\tilde{l}_1 = 0$. However, the amplification in mode 2 and the reservoir two-level atoms in the excited state gives $l_2 = 0$ and $\tilde{l}_2 = 2|\gamma_2|$. We note that, for standard PTSSs, amplification just compensates for damping, i.e., $\gamma_1 = -\gamma_2 \equiv \gamma$. However, we assume $\gamma_1 \equiv 2\gamma$ and $\gamma_2 \equiv 0$ for the analyzed passive PTSS. Similarly, we have $\gamma_1 \equiv 0$ and $\gamma_2 \equiv -2\gamma$ for the analyzed active PTSS. We also note that a more general PTSS containing also the nonlinear Kerr and cross-Kerr terms was analyzed in Refs. [11,12] using the method of small operator corrections to mean values. We note that, for the reservoir dynamics, we assume Markovian processes. However, the analysis can also be extended to non-Markovian dynamics. For example, a system coupled to a non-Markovian bath can be modeled by introducing an ancilla that is linearly coupled to the system and interacts with a standard Markovian reservoir. Such an approach enables the analysis of non-Markovian quantum exceptional points [49].

The Langevin-Heisenberg equations derived from the Hamiltonian \hat{H} in Eq. (1), with the help of the theory describing the system interaction with the reservoir, can conveniently be written in the following matrix form using the vectors $\hat{\mathbf{A}}^{\mathrm{T}} = (\hat{a}_1, \hat{a}_1^{\dagger}, \hat{a}_2, \hat{a}_2^{\dagger})$ and $\hat{\mathbf{L}}^{\mathrm{T}} = (\hat{l}_1, \hat{l}_1^{\dagger}, \hat{l}_2, \hat{l}_2^{\dagger})$:

$$\frac{d\hat{\mathbf{A}}(t)}{dt} = -i\mathbf{M}\hat{\mathbf{A}}(t) + \hat{\mathbf{L}}(t), \tag{3}$$

$$\mathbf{M} = \begin{bmatrix} -i\gamma_1 & 0 & \epsilon & \kappa \\ 0 & -i\gamma_1 & -\kappa & -\epsilon \\ \epsilon & \kappa & -i\gamma_2 & 0 \\ -\kappa & -\epsilon & 0 & -i\gamma_2 \end{bmatrix}. \tag{4}$$

In Eq. (3), we assume for simplicity real ϵ and κ .

We note that the model can readily be reformulated in terms of a master equation in the Lindblad form. Since it is naturally expressed in the coherent-state basis, this leads to a Fokker-Planck equation for the corresponding quasiprobability distribution. When assuming Gaussian states, the problem reduces to solving a set of ordinary differential equations for the first-order moments (mean amplitudes) and the second-order moments [the statistical coefficients defined later in Eq. (21)].

Introducing the evolution matrix P(t, t') [21],

$$\mathbf{P}(t, t') = \exp[-i\mathbf{M}(t - t')],\tag{5}$$

the solution of Eq. (3) is obtained as

$$\hat{\mathbf{A}}(t) = \mathbf{P}(t,0)\hat{\mathbf{A}}(0) + \hat{\mathbf{F}}(t), \tag{6}$$

$$\hat{\mathbf{F}}(t) = \int_0^t dt' \mathbf{P}(t, t') \hat{\mathbf{L}}(t'), \tag{7}$$

and $\hat{\mathbf{f}}^T \equiv (\hat{f}_1, \hat{f}_1^{\dagger}, \hat{f}_2, \hat{f}_2^{\dagger})$. The properties of the Langevin fluctuating operator forces in Eq. (2) result in the nonzero second-order correlation functions of the forces $\hat{\mathbf{f}}$ given as [21]

$$\langle \hat{\mathbf{F}}(t)\hat{\mathbf{F}}^{\dagger T}(t)\rangle = \int_0^t d\tilde{t} \int_0^t d\tilde{t}' \mathbf{P}(t,\tilde{t}) \langle \hat{\mathbf{L}}(\tilde{t})\hat{\mathbf{L}}^{\dagger T}(\tilde{t}')\rangle \mathbf{P}^{\dagger T}(t,\tilde{t}'),$$
(8)

where the symbol T stands for the transposed matrix.

According to Eq. (5), the eigenvectors of the evolution matrix **P** coincide with those of the dynamical matrix **M** and the corresponding eigenvalues $\Lambda_{\mathbf{P}}(t,t')$ are given as $\exp[-i\Lambda_{\mathbf{M}}(t-t')]$, where $\Lambda_{\mathbf{M}}$ contains the eigenvalues of matrix **M**. Diagonalization of the dynamical matrix **M** leaves us with the following eigenvectors and eigenvalues:

$$\mathbf{M} = \mathbf{T} \Lambda_{\mathbf{M}} \mathbf{T}^{-1}; \tag{9}$$

$$\Lambda_{\mathbf{M}} = -i\gamma_{+} \operatorname{diag}(1, 1, 1, 1) + \mu \operatorname{diag}(1, 1, -1, -1), \quad (10)$$

$$\mathbf{T} = (\mathbf{T}_{1}, \mathbf{T}_{2}, \mathbf{T}_{3}, \mathbf{T}_{4}),$$

$$\mathbf{T}_{1,2}^{\mathrm{T}} = \frac{1}{2\sqrt{\epsilon}} (\zeta^{\pm}, -\zeta^{\mp}, \pm \zeta^{\pm} \psi^{+}, \mp \zeta^{\mp} \psi^{+}),$$

$$\mathbf{T}_{3,4}^{\mathrm{T}} = \frac{1}{2\sqrt{\epsilon}} (\zeta^{\pm}, -\zeta^{\mp}, \mp \zeta^{\pm} \psi^{-}, \pm \zeta^{\mp} \psi^{-}),$$

$$\mathbf{T}^{-1} = (\mathbf{T}_{1}^{-1}, \mathbf{T}_{2}^{-1}, \mathbf{T}_{3}^{-1}, \mathbf{T}_{4}^{-1}),$$

$$\mathbf{T}_{1,2}^{-1\mathrm{T}} = \frac{\sqrt{\epsilon}}{2\sqrt{\mu}} (\zeta^{\pm} \psi^{-}, -\zeta^{\mp} \psi^{-}, \zeta^{\pm} \psi^{+}, -\zeta^{\mp} \psi^{+}),$$

$$\mathbf{T}_{3,4}^{-1\mathrm{T}} = \frac{\sqrt{\epsilon}}{2\sqrt{\mu}} (\zeta^{\pm}, \zeta^{\mp}, -\zeta^{\pm}, -\zeta^{\mp}),$$
(11)

and $\gamma_+ = (\gamma_1 + \gamma_2)/2$, $\gamma_- = (\gamma_1 - \gamma_2)/2$, $\xi = \sqrt{\epsilon^2 - \kappa^2}$, $\xi^\pm = \sqrt{\epsilon \pm \xi}$, $\mu = \sqrt{\epsilon^2 - \kappa^2 - \gamma_-^2}$, and $\psi^\pm = (\mu \pm i\gamma_-)/\xi$. We note that the structure of the eigenvectors and eigenvalues of the matrix \mathbf{M} closely resembles that obtained for the special case $\gamma_1 = -\gamma_2$ (\mathcal{PT} -symmetric case) analyzed in detail in Ref. [30] when studying the problem of nonclassicality and entanglement losses in the long-time limit caused by

fluctuating forces and related to the properties of the fluctuating forces.

According to Eq. (10) there exist two doubly degenerated eigenvalues

$$\nu_{1,2} = -i(\gamma_1 + \gamma_2)/2 \pm \sqrt{\epsilon^2 - \kappa^2 - (\gamma_1 - \gamma_2)^2/4}.$$
 (12)

We have the real eigenvalues $v_{1,2}^{ad}$ for the standard PTSS:

$$v_{1,2}^{\text{ad}} = \sqrt{\epsilon^2 - \kappa^2 - \gamma^2}.$$
 (13)

However, the eigenvalues $v_j^{\rm dd}$ ($v_j^{\rm aa}$) for the passive (active) PTSS additionally contain a common damping (amplification) factor γ ($-\gamma$):

$$v_{1,2}^{\rm dd} = -i\gamma \pm \sqrt{\epsilon^2 - \kappa^2 - \gamma^2},\tag{14}$$

$$v_{1,2}^{\text{aa}} = i\gamma \pm \sqrt{\epsilon^2 - \kappa^2 - \gamma^2}.$$
 (15)

Importantly, the eigenvectors of the matrix \mathbf{M} corresponding to the eigenvalues $\nu_{1,2}$ as given in Eq. (11) are identical for the standard, passive, and active PTSSs. This means that, when we express the system evolution in the basis of these eigenvectors, the dynamics in the three discussed PTSSs differ just by common multiplicative functions describing exponential damping in the passive PTSS and exponential amplification in the active PTSS. This property provides a strong foundation for a meaningful comparison of the statistical characteristics of the three systems discussed below. It also accounts for the fact that all three systems exhibit EPs at identical locations in the parameter space. The existence and degeneracies of these EPs, interpreted as Liouvillian EPs, were examined in detail in Ref. [39].

The solution of the Heisenberg equations (3) can then be written in the following form that explicitly expresses the symmetry contained in the above four-dimensional matrix formulation:

$$\hat{\mathbf{a}}(t) = \mathbf{U}(t)\hat{\mathbf{a}}(0) + \mathbf{V}(t)\hat{\mathbf{a}}^{\dagger}(0) + \hat{\mathbf{f}}(t). \tag{16}$$

In Eq. (16), we introduce $\hat{\mathbf{a}}^T \equiv (\hat{a}_1, \hat{a}_2), U_{j,k}(t) = P_{2j-1,2k-1}(t,0), V_{jk}(t) = P_{2j-1,2k}(t,0), \text{ and } \hat{f}_j(t) = \hat{F}_{2j-1}(t), j, k = 1, 2$. The matrices **U** and **V** attain the form

$$\mathbf{U}(t) = \frac{1}{\mu} \begin{bmatrix} \mu c(t) - \gamma_{-} s(t) & -i\epsilon s(t) \\ -i\epsilon s(t) & \mu c(t) + \gamma_{-} s(t) \end{bmatrix} \exp(-\gamma_{+} t),$$

$$\mathbf{V}(t) = -\frac{i\kappa s(t)}{\mu} \begin{bmatrix} 0 & 1\\ 1 & 0 \end{bmatrix} \exp(-\gamma_{+}t), \tag{17}$$

where $s(t) \equiv \sin(\mu t)$ and $c(t) \equiv \cos(\mu t)$.

Incorporation of the solution into Eq. (8) for the matrix $\langle \hat{\mathbf{F}}(t) \hat{\mathbf{F}}^{\dagger T}(t) \rangle$ of correlation functions of the fluctuating forces results in the following formulas for its elements:

$$\begin{split} \left\langle \hat{f}_{1}^{2}(t) \right\rangle &= (l_{2} + \tilde{l}_{2})\epsilon\kappa h(t)\theta, \\ \left\langle \hat{f}_{1}(t)\hat{f}_{1}^{\dagger}(t) \right\rangle &= [l_{1}h_{-}(t) - (\epsilon^{2}l_{2} + \kappa^{2}\tilde{l}_{2})h(t)]\theta, \\ \left\langle \hat{f}_{1}^{\dagger}(t)\hat{f}_{1}(t) \right\rangle &= [\tilde{l}_{1}h_{-}(t) - (\kappa^{2}l_{2} + \epsilon^{2}\tilde{l}_{2})h(t)]\theta, \\ \left\langle \hat{f}_{2}^{2}(t) \right\rangle &= (l_{1} + \tilde{l}_{1})\epsilon\kappa h(t)\theta, \\ \left\langle \hat{f}_{2}(t)\hat{f}_{2}^{\dagger}(t) \right\rangle &= [l_{2}h_{+}(t) - (\epsilon^{2}l_{1} + \kappa^{2}\tilde{l}_{1})h(t)]\theta, \\ \left\langle \hat{f}_{2}^{\dagger}(t)\hat{f}_{2}(t) \right\rangle &= [\tilde{l}_{2}h_{-}(t) - (\kappa^{2}l_{1} + \epsilon^{2}\tilde{l}_{1})h(t)]\theta, \end{split}$$

$$\langle \hat{f}_{1}(t)\hat{f}_{2}(t)\rangle = [l_{1}i\kappa d_{-}(t) + \tilde{l}_{2}i\kappa d_{+}(t)]\theta,$$

$$\langle \hat{f}_{2}(t)\hat{f}_{1}(t)\rangle = [\tilde{l}_{1}i\kappa d_{-}(t) + l_{2}i\kappa d_{+}(t)]\theta,$$

$$\langle \hat{f}_{1}^{\dagger}(t)\hat{f}_{2}(t)\rangle = [\tilde{l}_{1}i\epsilon d_{-}(t) - \tilde{l}_{2}i\epsilon d_{+}(t)]\theta,$$

$$\langle \hat{f}_{2}(t)\hat{f}_{1}^{\dagger}(t)\rangle = [l_{1}i\epsilon d_{-}(t) - l_{2}i\epsilon d_{+}(t)]\theta,$$
(18)

where $\theta = 1/(2\mu^2)$. We introduce the following functions in Eq. (18):

$$f(t) = \frac{1 - \exp(-2\gamma_{+}t) \exp(-2i\mu t)}{2(\gamma_{+} + i\mu)},$$

$$g(t) = [1 - \exp(-2\gamma_{+}t)]/(2\gamma_{+}),$$

$$h(t) = \operatorname{Re}\{f(t)\} - g(t),$$

$$h_{\pm}(t) = \operatorname{Re}\{(\mu \pm i\gamma_{-})^{2}f(t)\} + \xi^{2}g(t),$$

$$d_{\pm}(t) = \operatorname{Im}\{(\mu \pm i\gamma_{-})f(t)\} \mp \gamma_{-}g(t).$$
(19)

We note that we also have $\langle \hat{\mathbf{F}}(t) \rangle = \langle \hat{\mathbf{F}}^{\dagger}(t) \rangle = \mathbf{0}$.

IV. NONCLASSICALITY, ENTANGLEMENT, STEERING, AND BELL NONLOCALITY IN TWO-MODE BOSONIC SYSTEMS

In the analysis of nonclassicality and quantum correlations, we consider only the Gaussian states [20,45] that, however, represent the most useful states both in the analysis of fundamental physical experiments and applications. Moreover and most importantly, the linear Heisenberg-Langevin equations in Eq. (3) describe the state evolution inside this group of states. They are conveniently described by their normal characteristic function C_N written in the general form as [20,45]

$$C_{\mathcal{N}}(\mu_1, \mu_2, t) = \exp\left\{ \sum_{j=1,2} \left[(\alpha_j^*(t)\mu_j - \text{c.c.}) - B_j(t)|\mu_j|^2 + \frac{C_j(t)\mu_j^{2*} + \text{c.c.}}{2} \right] + [D(t)\mu_1^*\mu_2^* + \bar{D}(t)\mu_1\mu_2^* + \text{c.c.}] \right\}, \quad (20)$$

and c.c. replaces the complex conjugated term.

The parameters B_j , C_j , D, and \bar{D} that, together with the mode complex amplitudes, identify the state are obtained according to the formulas valid for the initial coherent states with amplitudes $\alpha_1(0)$ and $\alpha_2(0)$:

$$B_{j}(t) \equiv \langle \delta \hat{a}_{j}^{\dagger}(t) \delta \hat{a}_{j}(t) \rangle = \sum_{l=1,2} [|V_{jl}(t)|^{2} + \langle \hat{f}_{j}^{\dagger}(t) \hat{f}_{j}(t) \rangle],$$

$$C_{j}(t) \equiv \langle [\delta \hat{a}_{j}^{2}(t)]^{2} \rangle = \sum_{l=1,2} [U_{jl}(t) V_{jl}(t) + \langle \hat{f}_{j}^{2}(t) \rangle],$$

$$D(t) \equiv \langle \delta \hat{a}_{1}(t) \delta \hat{a}_{2}(t) \rangle$$

$$= \sum_{l=1,2} [U_{1l}(t) V_{2l}(t) + \langle \hat{f}_{1}(t) \hat{f}_{2}(t) \rangle],$$

$$\bar{D}(t) \equiv -\langle \delta \hat{a}_{1}^{\dagger}(t) \delta \hat{a}_{2}(t) \rangle$$

$$= -\sum_{l=1,2} [V_{1l}^{*}(t) V_{2l}(t) + \langle \hat{f}_{1}^{\dagger}(t) \hat{f}_{2}(t) \rangle],$$
(21)

where $\delta \hat{a}_j = \hat{a}_j - \langle \hat{a}_j \rangle$ for j = 1, 2. Substituting Eq. (17) into Eq. (21), we arrive at the formulas appropriate for our model:

$$B_{j}(t) = (\kappa/\mu)^{2} \tilde{s}(t) + \langle f_{j}^{\dagger}(t) f_{j}(t) \rangle,$$

$$C_{j}(t) = -(\epsilon \kappa/\mu^{2}) \tilde{s}(t) + \langle f_{j}^{2}(t) \rangle, \quad j = 1, 2,$$

$$D(t) = -i(\kappa/\mu) \tilde{c}(t) + i(\kappa \gamma_{+}/\mu^{2}) \tilde{s}(t) + \langle f_{1}(t) f_{2}(t) \rangle,$$

$$\bar{D}(t) = -\langle f_{1}^{\dagger}(t) f_{2}(t) \rangle, \tag{22}$$

where $\tilde{s}(t) = \sin^2(\mu t) \exp(-2\gamma_+ t)$, $\tilde{c}(t) = \sin(\mu t) \cos(\mu t) \exp(-2\gamma_+ t)$, and the correlation functions of the fluctuating forces are given in Eq. (18).

At an EP, we have $\mu = 0$ and the formulas (22) for the statistical parameters considerably simplify $(\mu \to 0)$:

$$B_{j}^{EP}(t) = \kappa^{2} t^{2} \exp(-2\gamma_{+}t) + \tilde{l}_{j} g(t)/2 - (\kappa^{2} l_{3-j}) + \epsilon^{2} \tilde{l}_{3-j}) \tilde{h}_{0}(t)/2,$$

$$C_{j}^{EP}(t) = -\epsilon \kappa t^{2} \exp(-2\gamma_{+}t) + (l_{3-j} + \tilde{l}_{3-j}) \epsilon \kappa \tilde{h}_{0}(t)/2,$$

$$j = 1, 2,$$

$$D^{EP}(t) = -i\kappa (t - \gamma_{+}t^{2}) \exp(-2\gamma_{+}t) + (l_{1} + \tilde{l}_{2}) i\kappa \times [t \exp(-2\gamma_{+}t) - g(t)]/(2\gamma_{+}) - (l_{1} - \tilde{l}_{2}) \times i\kappa \gamma_{-} \tilde{h}_{0}(t)/2,$$

$$\bar{D}^{EP}(t) = (\tilde{l}_{2} - \tilde{l}_{1}) i\epsilon [t \exp(-2\gamma_{+}t) - g(t)]/(2\gamma_{+}) + (\tilde{l}_{1} + \tilde{l}_{2}) i\epsilon \gamma_{-} \tilde{h}_{0}(t)/2,$$
(23)

where $\tilde{h}_0(t) \equiv [(t + \gamma_+ t^2) \exp(-2\gamma_+ t) - g(t)]/\gamma_+^2$. We can see that the original oscillatory behavior of the standard PTSS is replaced by the polynomial one at the EP. For the passive (active) PTSS additional exponential damping (amplification) occurs.

A. Nonclassicality

Coefficients of the quadratic terms in the argument of exponential function in Eq. (20) can be arranged into the matrix \mathbf{K}_{C_s} using the vector $(\mu_1, \mu_1^*, \mu_2, \mu_2^*)$. The matrix \mathbf{K}_{C_s} describes the characteristic function C_s written in the general s ordering of the field operators [20]

$$\mathbf{K}_{C_s}(s) = \frac{1}{2} \begin{bmatrix} -B_{1,s}(s) & C_1^* & \bar{D}^* & D\\ C_1 & -B_{1,s}(s) & D^* & \bar{D}\\ \bar{D} & D & -B_{2,s}(s) & C_2^*\\ D^* & \bar{D}^* & C_2 & -B_{2,s}(s) \end{bmatrix},$$
(24)

and $B_{j,s}(s) = (1-s)/2 + B_j$ for j = 1, 2. Eigenvalues of the matrix $\mathbf{K}_{C_s}(s)$, that depend on the ordering parameter s, bear the information about the state nonclassicality [19,28]. Detailed analysis reveals that the Lee nonclassicality depth τ [30,33] of the state is equal to the greatest positive eigenvalue of the matrix $\mathbf{K}_{C_s}(s = 1)$ written for the normal field-operator ordering. Applying this procedure to the individual modes, we immediately arrive at the formula for the local nonclassicality depths τ_j for j = 1, 2:

$$\tau_i = \max\{0, |C_i| - B_i\}. \tag{25}$$

B. Steering

Quantum correlations of the Gaussian states are described by their coherence matrix σ defined for the vector $(\hat{q}_1, \hat{p}_1, \hat{q}_2, \hat{p}_2)$ [45]:

$$\sigma = \begin{bmatrix} \sigma_{1} & \sigma_{12} \\ [\sigma_{12}]^{T} & \sigma_{2} \end{bmatrix},$$
(26)
$$\sigma_{j} = \begin{bmatrix} 1 + 2B_{j} + 2\operatorname{Re}\{C_{j}\} & 2\operatorname{Im}\{C_{j}\} \\ 2\operatorname{Im}\{C_{j}\} & 1 + 2B_{j} - 2\operatorname{Re}\{C_{j}\} \end{bmatrix},$$

$$\sigma_{12} = 2 \begin{bmatrix} \operatorname{Re}\{D - \bar{D}\} & \operatorname{Im}\{D - \bar{D}\} \\ \operatorname{Im}\{D + \bar{D}\} & -\operatorname{Re}\{D + \bar{D}\} \end{bmatrix},$$
(27)

where $\hat{q}_j = (\hat{a}_j + \hat{a}_j^{\dagger})/2$, $\hat{p}_j = (\hat{a}_j - \hat{a}_j^{\dagger})/(2i)$, j = 1, 2. The steering of mode (3 - j) by mode j for j = 1, 2 is then expressed using the formula [36]

$$S_{i \to 3-i} = \max\{0, \det\{\sigma_i\}/\det\{\sigma\}\}/2.$$
 (28)

C. Entanglement

The (logarithmic) negativity E_N [34,35] as a commonly accepted measure of entanglement is inferred from the coherence matrix σ^{PT} defined for the vector $(\hat{q}_1, \hat{p}_1, \hat{q}_2, -\hat{p}_2)$, i.e., for the partially transposed state of mode 2 [50–52]

$$\sigma^{PT} = \begin{bmatrix} \sigma_{1} & \sigma_{12}^{PT} \\ \left[\sigma_{12}^{PT}\right]^{T} & \sigma_{2}^{PT} \end{bmatrix}, \tag{29}$$

$$\sigma_{2}^{PT} = \begin{bmatrix} 1 + 2B_{2} + 2\operatorname{Re}\{C_{2}\} & -2\operatorname{Im}\{C_{2}\} \\ -2\operatorname{Im}\{C_{2}\} & 1 + 2B_{2} - 2\operatorname{Re}\{C_{2}\} \end{bmatrix},$$

$$\sigma_{12}^{PT} = 2 \begin{bmatrix} \operatorname{Re}\{D - \bar{D}\} & \operatorname{Im}\{-D + \bar{D}\} \\ \operatorname{Im}\{D + \bar{D}\} & \operatorname{Re}\{D + \bar{D}\} \end{bmatrix}. \tag{30}$$

The symplectic eigenvalue ν_{-} determined with the help of the invariants Δ and δ [45]

$$\nu_{-} = \sqrt{\frac{\delta}{2} - \sqrt{\frac{\delta^{2}}{4} - \Delta}},$$

$$\Delta = \det\{\sigma^{PT}\},$$

$$\delta = \det\{\sigma_{1}\} + \det\{\sigma_{2}^{PT}\} + 2\det\{\sigma_{12}^{PT}\},$$
(31)

then gives the negativity

$$E_N = \max\{0, -\ln(\nu_-)\}. \tag{32}$$

D. Bell nonlocality

The strongest quantum correlations, that imply the Bell nonlocality, are quantified by the Bell parameter B_{Bell} [37] that is in our case a specific linear combination of the mean values of suitably displaced parity operators $\hat{\Pi}(\beta_1, \beta_2)$. Introducing two sets of displacements (β_1, β_2) and (β_1', β_2') the Bell parameter B_{Bell} is determined along the formula

$$B_{\text{Bell}}(\beta_1, \beta_2; \beta_1', \beta_2') = \langle \hat{\Pi}(\beta_1, \beta_2) \rangle + \langle \hat{\Pi}(\beta_1', \beta_2) \rangle + \langle \hat{\Pi}(\beta_1, \beta_2') \rangle - \langle \hat{\Pi}(\beta_1', \beta_2') \rangle.$$
(33)

If $|B_{\text{Bell}}| > 2$ for any suitable choice of the displacements (β_1, β_2) and (β_1', β_2') , the state exhibits the Bell nonlocality manifested by the violation of the Bell inequalities [37]. According to Refs. [53,54], the mean value of a displaced parity

operator is directly obtained from the Wigner function $\Phi_{s=0}$ using the formula

$$\langle \hat{\Pi}(\beta_1, \beta_2) \rangle = \frac{\pi^2}{4} \Phi_{s=0}(\beta_1, \beta_2). \tag{34}$$

To reveal the Wigner function $\Phi_{s=0}$, we first have to rewrite the matrix $\mathbf{K}_{C_s}(s=0)$ into that written for the vector $\boldsymbol{\mu}^{\text{real},T} \equiv (\text{Re}\{\mu_1\}, \text{Im}\{\mu_1\}, \text{Re}\{\mu_2\}, \text{Im}\{\mu_2\})$:

$$\mathbf{K}_{C_{s}}^{\text{real}} = \begin{bmatrix} -B_{1,s}(0) + \text{Re}\{C_{1}\} & \text{Im}\{C_{1}\} \\ \text{Im}\{C_{1}\} & -B_{1,s}(0) - \text{Re}\{C_{1}\} \\ \text{Re}\{D + \bar{D}\} & \text{Im}\{D - \bar{D}\} \\ \text{Im}\{D + \bar{D}\} & \text{Re}\{-D + \bar{D}\} \end{bmatrix}$$

$$\frac{\text{Re}\{D + \bar{D}\}}{\text{Im}\{D - \bar{D}\}} & \frac{\text{Im}\{D + \bar{D}\}}{\text{Re}\{-D + \bar{D}\}}$$

$$-B_{2,s}(0) + \text{Re}\{C_{2}\} & \frac{\text{Im}\{C_{2}\}}{\text{Im}\{C_{2}\}} & \text{Im}\{C_{2}\} \end{bmatrix}. (35)$$

Forming the vector $\boldsymbol{\alpha}^{\text{real},T} \equiv (\text{Im}\{\alpha_1\}, \text{Re}\{\alpha_1\}, \text{Im}\{\alpha_2\}, \text{Re}\{\alpha_2\})$ from the arguments α_1 and α_2 of the Wigner function $\Phi_{s=0}(\alpha_1,\alpha_2)$ the four-dimensional Fourier transform of the characteristic function $C_{s=0}(\boldsymbol{\alpha}^{\text{real},T})$ related to the symmetric ordering of field operators leaves the Wigner function in the form

$$\Phi_{s=0}(\alpha_1, \alpha_2) = \frac{\exp\left[\boldsymbol{\alpha}^{\text{real}, T} \mathbf{K}_{C_s}^{\text{real}, -1} \boldsymbol{\alpha}^{\text{real}}\right]}{\pi^2 \sqrt{\det\{\mathbf{K}_{C_s}^{\text{real}}\}}}.$$
 (36)

In Eq. (36), we use the inverse to the matrix $\mathbf{K}_{C_s}^{\text{real}}$ and its determinant.

The Bell parameter B_{Bell} depends on two sets of displacements that have to be suitably chosen to reveal the violation of the Bell inequalities. In the numerical analysis, inspired by Refs. [53,55,56], we set $(\beta_1, \beta_2) = (0, 0)$ and systematically scan the remaining complex displacements (β_1', β_2') (expressed in radial coordinates) such that $|\beta_j'| \leq 2\sqrt{B_{j,s}(0)}$ for j = 1, 2.

V. ROLE OF \mathcal{PT} -SYMMETRY IN NONCLASSICAL-STATE GENERATION

Before diving into a detailed discussion of the system's behavior, it is important to note that its dynamics, particularly regarding damping and amplification, are shaped by two competing effects. The first involves the influence of damping or amplification on the coherent component of the system's evolution. In this context, amplification is generally considered beneficial compared to damping, as it increases mode amplitudes. This increase, in turn, enhances the system's effective physical nonlinearity, defined as the product of the nonlinear coupling constant and the mode amplitudes.

The second effect stems from random fluctuating forces (i.e., quantum noise) that tend to degrade nonclassical features and quantum correlations by disrupting phase coherence within the system. Notably, the noise accompanying amplification is generally stronger than that associated with damping, due in part to spontaneous photon emission from reservoir atoms in excited states.

In detail, mutual balance between damping and amplification in standard PTSSs gives their specific dynamical

behavior. In our case, \mathcal{PT} symmetry is reached assuming $\gamma_1=\gamma,\ \gamma_2=-\gamma,\ l_1=2\gamma,\ \tilde{l}_2=2\gamma,\ \tilde{l}_1=l_2=0.$ In specific cases, at EPs, spectral degeneracies of the dynamical matrix \mathbf{M} occur being accompanied by the corresponding eigenvector degeneracies. This means that the system evolution considerably simplifies and only a single eigenfrequency is sufficient to describe the evolution. Following Eq. (10), or Eq. (13), such situation occurs provided that $\mu\equiv\sqrt{\epsilon^2-\kappa^2-\gamma^2}=0$. For the Hamiltonian \hat{H} in Eq. (1) and assuming $\gamma_1=-\gamma_2=\gamma$, EPs occur for

$$\frac{\kappa^2}{\epsilon^2} + \frac{\gamma^2}{\epsilon^2} = 1. \tag{37}$$

In the analyzed system, this specific dynamics influences the ability to generate nonclassical states of different kinds. The nonclassicality of a generated state reflects either local nonclassicalities of the constituting modes 1 and 2 or quantum correlations between these modes. Whereas we quantify below the nonclassicalities by the corresponding Lee nonclassicality depths τ , τ_1 , and τ_2 , quantum correlations with the increasing quantumness are in turn quantified by the negativity E_N (entanglement), steering parameters $S_{1\rightarrow 2}$ and $S_{2\rightarrow 1}$ (steering), and the Bell parameter (Bell nonlocality).

We examine the system behavior by assuming the modes initially in their vacuum states (arbitrary initial coherent states in both modes can be considered as well) and follow their temporal evolution. To assess the behavior of the investigated quantities, we determine their maximal values along the time t axis

$$\tau = \max_{t\epsilon} \{\tau(t\epsilon)\}, \quad E_N = \max_{t\epsilon} \{E_N(t\epsilon)\},$$

$$\tau_j = \max_{t\epsilon} \{\tau_j(t\epsilon)\}, \quad S_{j\to 3-j} = \max_{t\epsilon} \{S_{j\to 3-j}(t\epsilon)\},$$

$$B_{\text{Bell}} = \max_{t\epsilon} \{B_{\text{Bell}}(t\epsilon)\},$$
(38)

where j=1,2 and compare these maximal values for the whole parameter space of the investigated system. We note that, due to linearity of the corresponding Heisenberg equations, the parameter space is effectively two-dimensional and is spanned by the variables κ/ϵ and γ/ϵ .

To reveal the role of balance between damping and amplification in the standard PTSS, we compare its behavior with two specific cases (systems) in which only damping $(\gamma_1 = \gamma, \gamma_2 = 0, l_1 = 2\gamma, \tilde{l}_1 = l_2 = \tilde{l}_2 = 0)$ and only amplification $(\gamma_1 = 0, \gamma_2 = -\gamma, \tilde{l}_2 = 2\gamma, l_1 = \tilde{l}_1 = l_2 = 0)$ influence the system dynamics. Both systems for comparison, owing to their physical nonlinearities, preserve the ability to generate the nonclassical states. Mutual comparison of the maximal values of the quantities characterising both nonclassicality and different types of quantum correlations then sheds light on how beneficial the balance between damping and amplification in standard PTSSs is when generating the nonclassical states. We note that in the systems for comparison different conditions for EPs occur:

$$\frac{\kappa^2}{\epsilon^2} + \frac{\gamma^2}{4\epsilon^2} = 1. \tag{39}$$

The change of the system dynamics caused by the absence of amplification even results in the observation of nonclassical properties of the modes in the asymptotic limit $t \to \infty$ [$t\epsilon \to \infty$]. In this case, only the following coeffi-

cients from Eq. (22) attain asymptotically nonzero values

$$B_2(\infty) = \frac{\kappa^2}{\epsilon^2 - \kappa^2}, \quad C_2(\infty) = -\frac{\epsilon \kappa}{\epsilon^2 - \kappa^2}.$$
 (40)

They imply the nonclassicality in mode 2 quantified by the nonclassicality depth τ_2 :

$$\tau_2(\infty) = \frac{\kappa}{\epsilon + \kappa}.\tag{41}$$

A. Nonclassicality

As documented in Figs. 2(a) to 2(d), (first row), the analyzed standard PTSS allows for the generation of highly nonclassical states with τ , τ_1 , $\tau_2 \rightarrow 1/2$ for small γ/ϵ and κ/ϵ close to 1, i.e., when the system damping and amplification are small. We note that 1/2 gives the greatest value of nonclassicality depth attained by a Gaussian state. As the nonlinear coupling constant κ represents the source of nonclassicality, the greater the value of κ is the better the ability of the system to generate nonclassical states is. Despite the balance between damping and amplification, the greater the damping and amplification are the worse the system ability to provide nonclassical states is. This is because stronger damping and amplification are accompanied by more intense fluctuating forces. This relationship is quantified by the fluctuation-dissipation and fluctuation-amplification theorems [43]. These fluctuating forces then weaken the system ability to generate nonclassical states. We can see in Fig. 2(b) that we also reach greatest field intensities n^{ad} in the area of parameters optimal for nonclassical-state generation.

The comparison of maximal values of the nonclassicality depths τ and τ_1 with those characterizing the systems with only damping [see Figs. 2(a) and 2(c), (second row)] and only amplification [see Figs. 2(a) and 2(c), (third row)] leads us to the conclusion that both systems for comparison provide greater maximal values than those of the corresponding standard PTSS for most system parameters. The only exception is the narrow region in the graph of the ratio $\tau_1^{\rm ad}/\tau_1^{\rm d}$ of nonclassicality depths [see Fig. 2(c), second row] for values of κ/ϵ close to 1. In this region, a large nonlinear coupling constant κ , combined with the high amplitudes of the amplified mode 2 in the standard PTSS, leads to enhanced effective physical nonlinearity. This, in turn, results in stronger nonclassicality compared to the case without the amplified mode 2. Notably, this region naturally occurs near the curve of EPs and within the domain of exponential mode amplitude growth, in contrast to the periodic amplitude behavior observed in the \mathcal{PT} -symmetric region.

However, for fixed model parameters, the nonclassicality depth τ_2 of mode 2 is highest for the system with only damping [see Fig. 2(d), (second row)] and lowest for the system with only amplification [see Fig. 2(d), (third row)]. Moreover, in the area of parameters optimal for nonclassical-state generation, both systems for comparison give more intense (and more nonclassical) nonclassical states.

B. Entanglement and steering

The analysis of entanglement quantified by the negativity E_N and steering described by the steering parameters

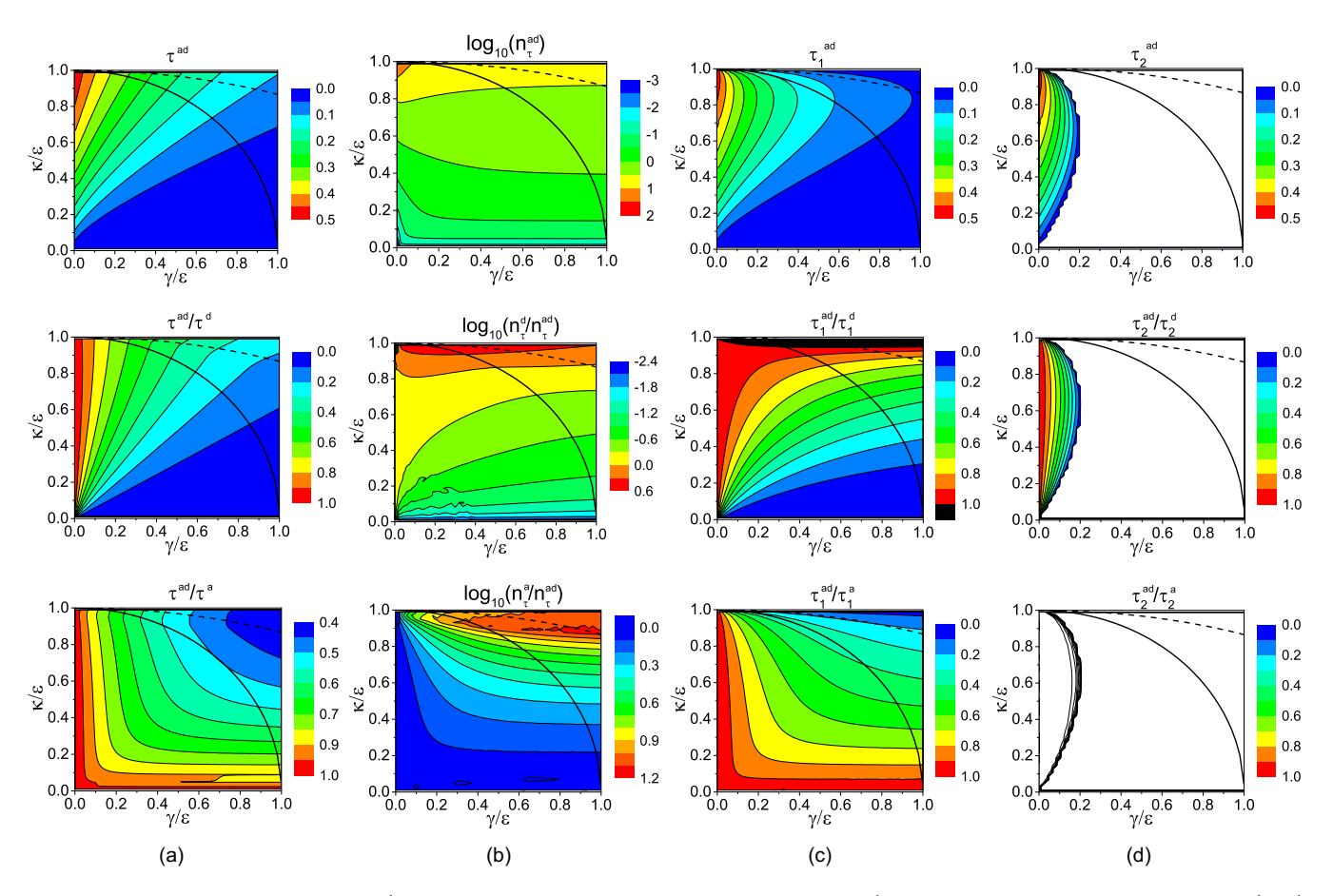


FIG. 2. (a) Nonclassicality depth $\tau^{\rm ad}$ and (b) the corresponding mean photon number $n_{\tau}^{\rm ad}$, (c), [(d)] local nonclassicality depth $\tau_1^{\rm ad}$ [$\tau_2^{\rm ad}$] of mode 1 [2] of standard PTSS as they depend on model parameters γ/ϵ and κ/ϵ . The values of the drawn parameters are compared with those originating in the model with considered only damping (superscript d) and only amplification (superscript a). In white areas, $\tau_2^{\rm ad} = 0$. Solid (dashed) black curves identify positions of EPs in PTSS (systems with only damping and only amplification). The superscript notation is explained in Fig. 1.

 $S_{1\rightarrow2}$ and $S_{2\rightarrow1}$ provides us the graphs in Figs. 3(a) to 3(d), (first row) for the standard PTSS and the graphs in Figs. 3(a) to 3(d), (second row) when the system with only damping is considered and the graphs in Figs. 3(a) to 3(d), (third row) when the system with only amplification is addressed. The conclusions drawn from these graphs are similar to the above ones for the nonclassicality depth τ : Both systems for comparison allow for greater values of the negativity E_N and the steering parameters $S_{1\rightarrow2}$ and $S_{2\rightarrow1}$ than the standard PTSS. We note that, whereas greater nonlinearity constant κ/ϵ and small damping and amplification constants are required to allow steering of the amplified mode 2 by the damped mode 1, the amplified mode 2 steers the damped mode 1 for any value of the system parameters.

C. Bell nonlocality

The advantage of the system with only damping in nonclassicality-state generation over the other two investigated systems manifests dramatically when generating the states that exhibit the Bell nonlocality. Only this system allows to violate the Bell inequalities in the wide area of the system parameters: Only the small nonlinearity constant κ/ϵ and greater damping and amplification constants γ/ϵ prevent from

the violation of the Bell inequalities [see Fig. 4(a)]. Contrary to this, only very small values of damping and amplification constants γ/ϵ are compatible with the states violating the Bell inequalities in the standard PTSS and its variant with only amplification [see Figs. 4(b) and 4(c), $\gamma/\epsilon < 0.03$]. Even under these conditions the attained values of the Bell parameters $B_{\rm Bell}^{\rm ad}$ and $B_{\rm Bell}^{\rm a}$ are smaller than the parameters $B_{\rm Bell}^{\rm d}$ belonging to the system with only damping.

In summary, the coexistence of damping and amplification under balanced conditions in the standard PTSS offers a clear advantage only when the nonlinear coupling constant κ is large. In this case, the increased amplitudes of the amplified mode 2 enhance the system's effective physical nonlinearity, leading to higher nonclassicality depths τ_1 for the damped mode 1. However, from the perspective of other quantumness quantifiers, such as the global nonclassicality depth, negativity, steering parameters, and the Bell nonlocality parameter, this balance provides no significant benefit.

VI. ROLE OF QUANTUM FLUCTUATIONS IN NONCLASSICAL-STATE GENERATION

Parallel eigenvalue analysis of the dynamical matrices **M** of the standard PTSS [damping constant $\gamma_1 = \gamma$ and

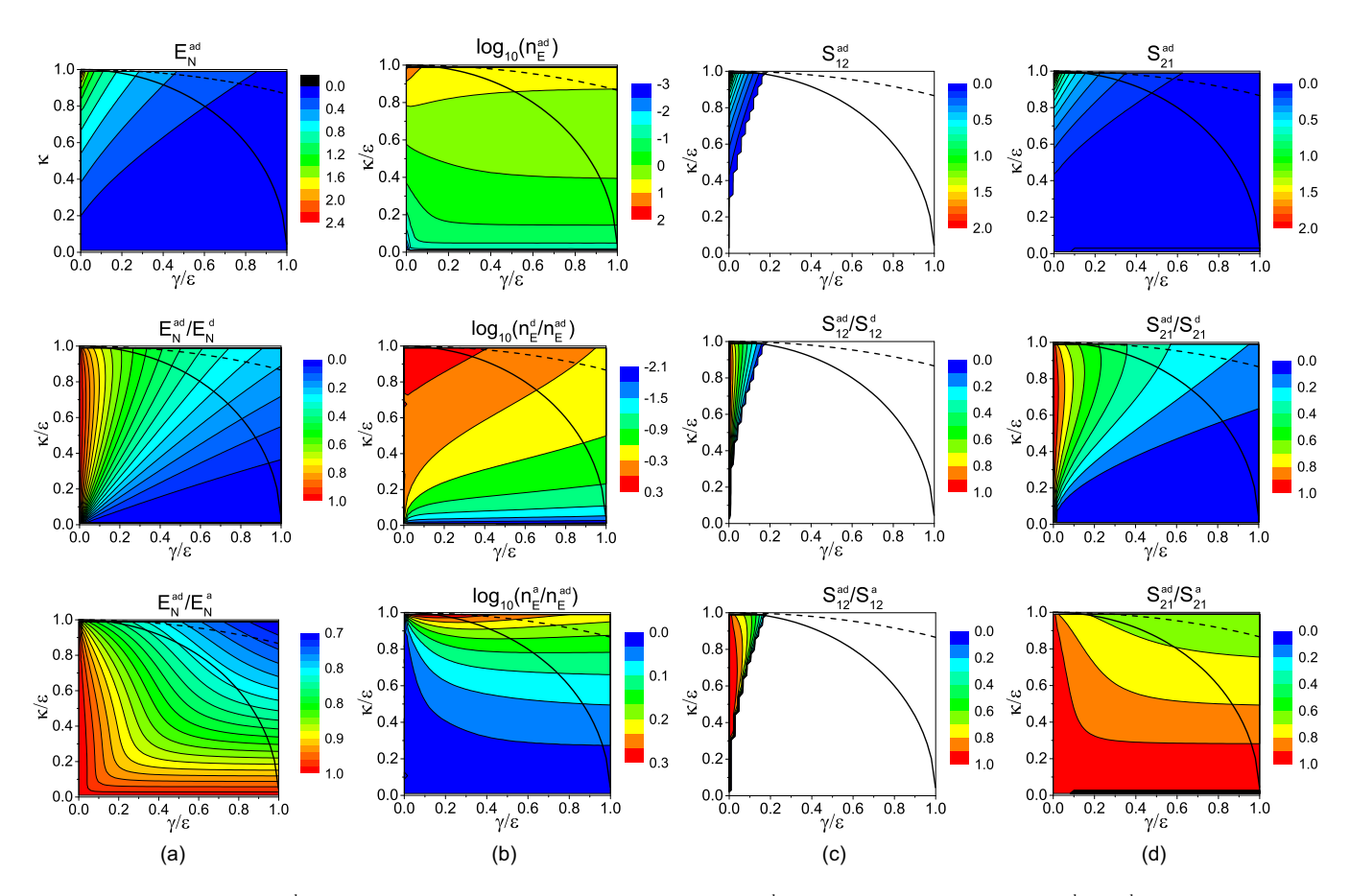


FIG. 3. (a) Negativity $E_N^{\rm ad}$ and (b) the corresponding mean photon number $n_E^{\rm ad}$, (c), [(d)] steering parameter $S_{1\to 2}^{\rm ad}$ [$S_{2\to 1}^{\rm ad}$] of standard PTSS as they depend on model parameters γ/ϵ and κ/ϵ . The values of the drawn parameters are compared with those originating in the model with considered only damping (superscript d) and only amplification (superscript a). In white areas, $S_{1\to 2}^{\rm ad}=0$. Solid (dashed) black curves identify positions of EPs in PTSS (systems with damping and amplification). The superscript notation is explained in Fig. 1.

amplification constant $\gamma_2 = -\gamma$, for the eigenvalues, see Eq. (13)], passive PTSS [damping constant $\gamma_1 = 2\gamma$ and no amplification $\gamma_2 = 0$, $l_1 = 4\gamma$, $\tilde{l}_1 = l_2 = \tilde{l}_2 = 0$, see Eq. (14)], and active PTSS [no damping $\gamma_1 = 0$ and amplification constant $\gamma_2 = -2\gamma$, $\tilde{l}_2 = 4\gamma$, $l_1 = \tilde{l}_1 = l_2 = 0$, see Eq. (15)] reveals striking similarity.

Their eigenfrequencies $\Lambda_{\mathbf{M}}$ differ just by their imaginary parts common to all eigenvalues: Whereas the imaginary part of Λ_M is zero for the standard PTSS, it gives the average damping constant γ for the passive system and the average amplification constant $-\gamma$ for the active system. Also, as already discussed in Sec. III, the corresponding eigenvectors are the same. We note that detailed analysis of such behavior is given in Ref. [31]. This similarity means that, for the same initial conditions for modes 1 and 2, the evolution of operator amplitudes of the passive [active] system differs from that of the standard PTSS just by the multiplicative function $\exp(-\gamma t) [\exp(\gamma t)]$. When the coefficients of the normal characteristic function C_N given in Eq. (22) are considered the multiplicative factors are $\exp(-2\gamma t) [\exp(2\gamma t)]$. It is not only this coherent dynamics that causes different evolution of the three PTSS. The dynamics of these systems differ also because of different properties of their fluctuating operator forces \hat{l}_i and \hat{l}_i^{\dagger} , j = 1, 2, prescribed to the modes in Eq. (2). Specifically, the properties of fluctuating forces assigned to the modes with amplification have more detrimental influence

to the nonclassical-state generation than those belonging to the modes with damping because of spontaneous emission in the reservoir modes [17]. We note that, when a mode is neither damped nor amplified no fluctuating forces are required to comply with the rules of quantum mechanics.

Detailed comparison of the properties of modes in these three systems is provided in Fig. 5 by determining the maximal values of the nonclassicality depths τ , τ_1 , and τ_2 and Fig. 6 by plotting the maximal values of the negativity E_N and the steering parameters $S_{1\rightarrow 2}$ and $S_{2\rightarrow 1}$. We note that, in the passive PTSS, mode 2 is asymptotically nonclassical and the corresponding parameters including the nonclassicality depth τ_2 are given in Eqs. (40) and (41).

A. Comparison with passive \mathcal{PT} -symmetric system

According to Figs. 5(a) to 5(d), (first row), the nonclassicality depths τ and τ_2 are always smaller for the standard PTSS compared to those of the passive one. This is true also for the nonclassicality depth τ_1 for κ/ϵ smaller than approx. 0.6. Greater values of τ_1 for the standard PTSS than those for the passive one are reached only for κ/ϵ greater than approx. 0.6. This is so, because doubled damping of mode 1 does not provide enough time for nonclassical-state generation for greater nonlinear coupling constants κ/ϵ . Moreover, in the standard PTSS, the amplified mode 2 results in larger mode-2

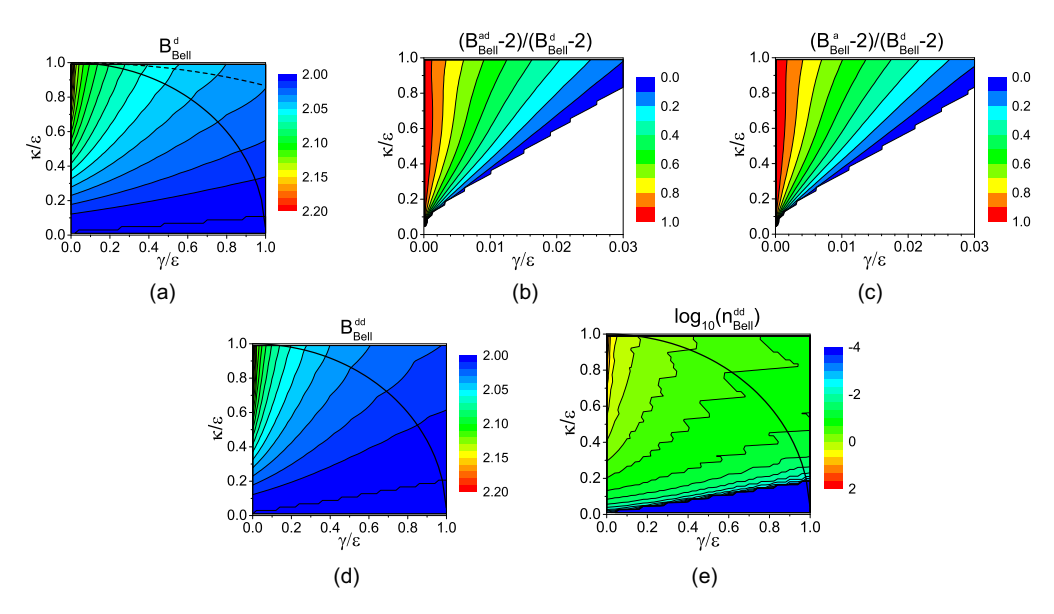


FIG. 4. (a) Bell parameter $B_{\rm Bell}^{\rm d}$, (b) [(c)] ratio $(B_{\rm Bell}^{\rm ad}-2)/(B_{\rm Bell}^{\rm d}-2)$ [$(B_{\rm Bell}^{\rm a}-2)/(B_{\rm Bell}^{\rm d}-2)$] of Bell parameters, (d) Bell parameter $B_{\rm Bell}^{\rm dd}$ and the corresponding mean photon number $n_{\rm Bell}^{\rm dd}$ as they depend on model parameters γ/ϵ and κ/ϵ . In white areas, the Bell inequalities are not violated ($B_{\rm Bell}=2$). Solid [dashed] black curves identify positions of EPs in PTSS as well as systems with doubled damping and amplification (systems with damping and amplification). The superscript notation is explained in Fig. 1.

amplitudes, which in turn enhance the effective physical non-linearity. The standard PTSS also provides the nonclassical states with greater overall intensities compared to those of the passive PTSS, excluding the area of parameters with κ/ϵ above 0.8 [see Fig. 5(b), (first row)]. The comparison of the behavior of quantum correlations described by the negativity and steering parameters as presented in Figs. 6(a) to 6(d), (first row) is even more straightforward. The standard PTSS always

gives smaller maximal values of the negativity E_N and the steering parameters $S_{1\rightarrow 2}$ and $S_{2\rightarrow 1}$ and the states with smaller overall intensities. In the passive PTSS, the states violating the Bell inequalities are generated in the wide area of the system parameters, similarly as in the damped part of the standard system [compare Figs. 4(d) and 4(a)]. These states also attain greater overall intensities, as documented in Fig. 4(e). This contrasts with the behavior of the standard PTSS that provides

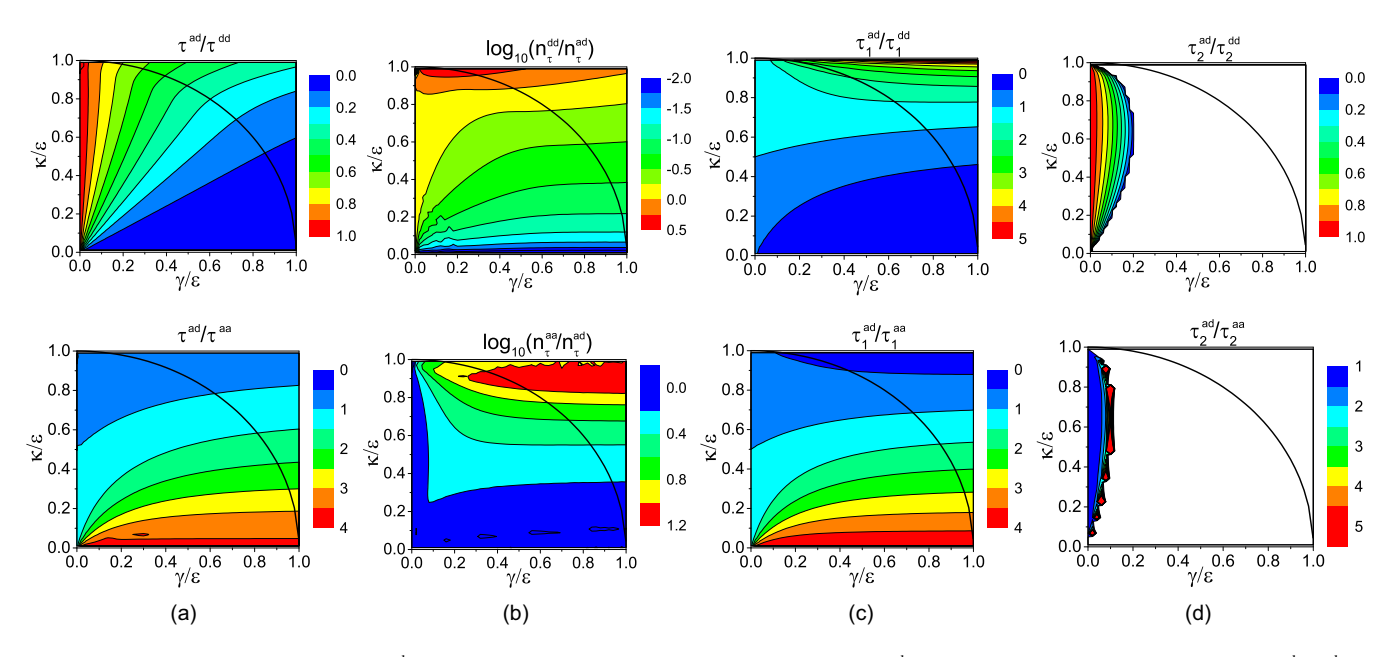


FIG. 5. (a) Nonclassicality depth τ^{ad} and (b) the corresponding mean photon number n_{τ}^{ad} , (c), [(d)] local nonclassicality depth τ_{1}^{ad} [τ_{2}^{ad}] of mode 1 [2] of standard PTSS relative to the values of passive PTSS with only doubled damping (superscript dd) and active PTSS with only doubled amplification (superscript aa) as they depend on model parameters γ/ϵ and κ/ϵ . In white areas, $\tau_{2}^{ad}=0$. Solid black curves identify positions of EPs in PTSS as well as systems with only doubled damping and only doubled amplification. The superscript notation is explained in Fig. 1.

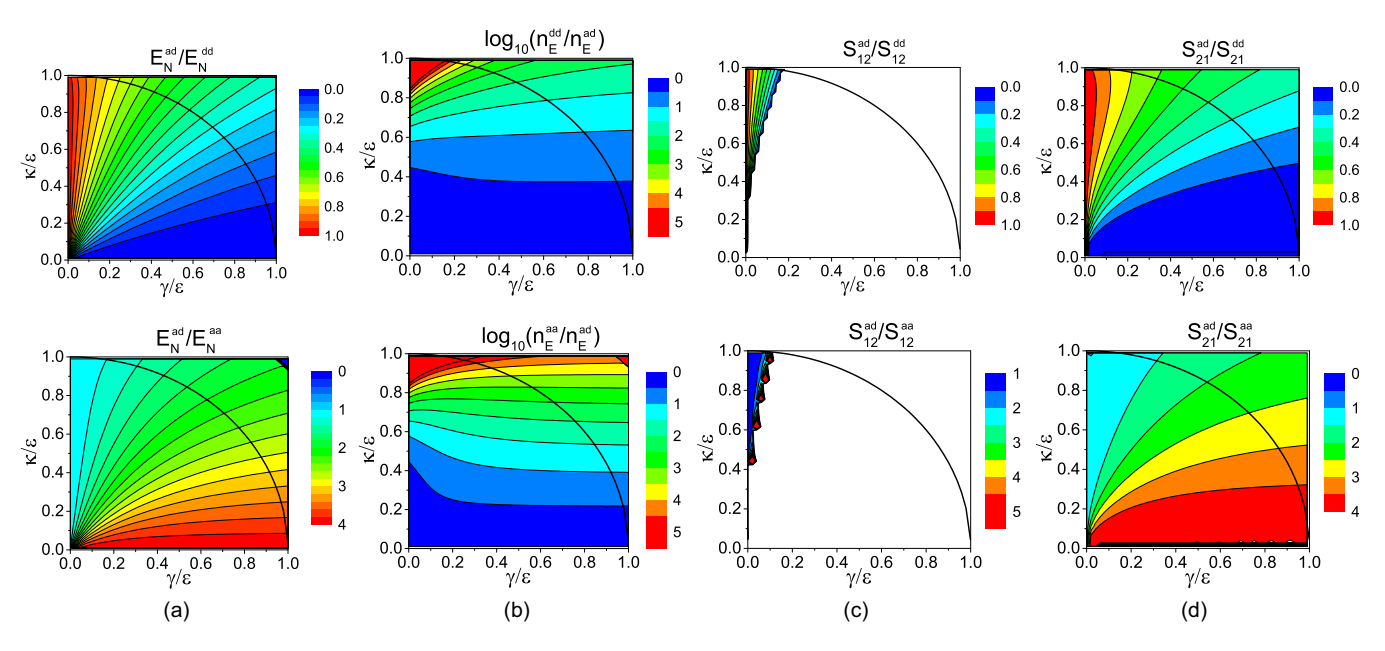


FIG. 6. (a) Negativity $E_N^{\rm ad}$ and (b) the corresponding mean photon number $n_E^{\rm ad}$, (c), [(d)] steering parameter $S_{1\to 2}^{\rm ad}$ [$S_{2\to 1}^{\rm ad}$] of standard PTSS relative to the values of passive PTSS (superscript dd), and active PTSS (superscript aa) as they depend on model parameters γ/ϵ and κ/ϵ . In white areas, $S_{1\to 2}^{\rm ad}=0$. Solid black curves identify positions of EPs in PTSS as well as systems with doubled damping and amplification. The superscript notation is explained in Fig. 1.

such states only for very small values of the damping and amplification constants γ . This behavior qualitatively originates in the stronger detrimental effects of the fluctuating forces in the amplified mode of the standard PTSS compared to those of mode 2 of the passive system (no amplification).

B. Comparison with active \mathcal{PT} -symmetric system

Stronger fluctuating forces in the active PTSS imply in general worse conditions for the nonclassical-state generation compared to the standard PTSS. Indeed, the graphs in Figs. 5(a) to 5(d), (second row) giving the maximal values of nonclassicality depths τ , τ_1 , and τ_2 confirm this. Only when κ/ϵ is greater than approx. 0.6 mode 1 in the active system (no damping) attains greater nonclassicality depths τ_1 compared to the damped mode 1 of the standard PTSS. This effect is due to the higher effective physical nonlinearity of the active PTSS, which arises from its larger mode amplitudes. This behavior of mode 1 also results in greater maximal values of the global nonclassicality depth τ of the active PTSS compared to those of the standard one in certain subarea around $\kappa/\epsilon = 1$. In general the active PTSS gives greater overall intensities of the generated nonclassical states. As for quantum correlations and opposed to what was written when comparing with the passive PTSS, the standard PTSS always gives greater maximal values of the negativity E_N as well as the steering parameters $S_{1\rightarrow 2}$ and $S_{2\rightarrow 1}$. However the nonclassical states attain smaller overall intensities than those reached in the active PTSS [see Fig. 6(b), (second row)]. The ability of both systems to generate the states with the Bell nonlocality is very weak and it is restricted to very low values of the damping and amplification constants γ/ϵ .

We note that, in the above calculations, we assumed the reservoir two-level atoms in the ground states to consistently describe damping and in the excited states to consistently describe amplification. Nevertheless, the two-level reservoir atoms for damping can partly be in their excited states similarly as the reservoir two-level atoms for amplification can partly be in their ground states. These modifications of the reservoir properties make closer the behavior of the above considered standard, passive, and active PTSSs. In the asymptotic limit of equally populated ground and excited levels of the atoms in both reservoirs, the behavior of all PTSSs is identical.

VII. QUANTUMNESS AND HIERARCHY OF QUANTUM CORRELATIONS

The results presented above about the system's nonclassicality and its quantum correlations, made systematically across the entire hierarchy of quantum correlations (entanglement, steering, and Bell nonlocality), show that the balance between damping and amplification in the standard PTSS, and the ensuing specific system dynamics, do not improve, except for minor cases, the system's ability to generate nonclassical states exhibiting different kinds of quantumness. We note that similar hierarchies of quantumness potentials were studied in Refs. [32,57], in the context of single-qubit states.

In general, the set of states exhibiting the Bell nonlocality forms a subset of the set of steerable states. Similarly, steerable states constitute a subset of entangled states. Finally, all entangled states belong to the class of nonclassical states, together with those exhibiting only local nonclassicality. This hierarchy of quantum states, classified according to different forms of quantumness, is also preserved for the quantities

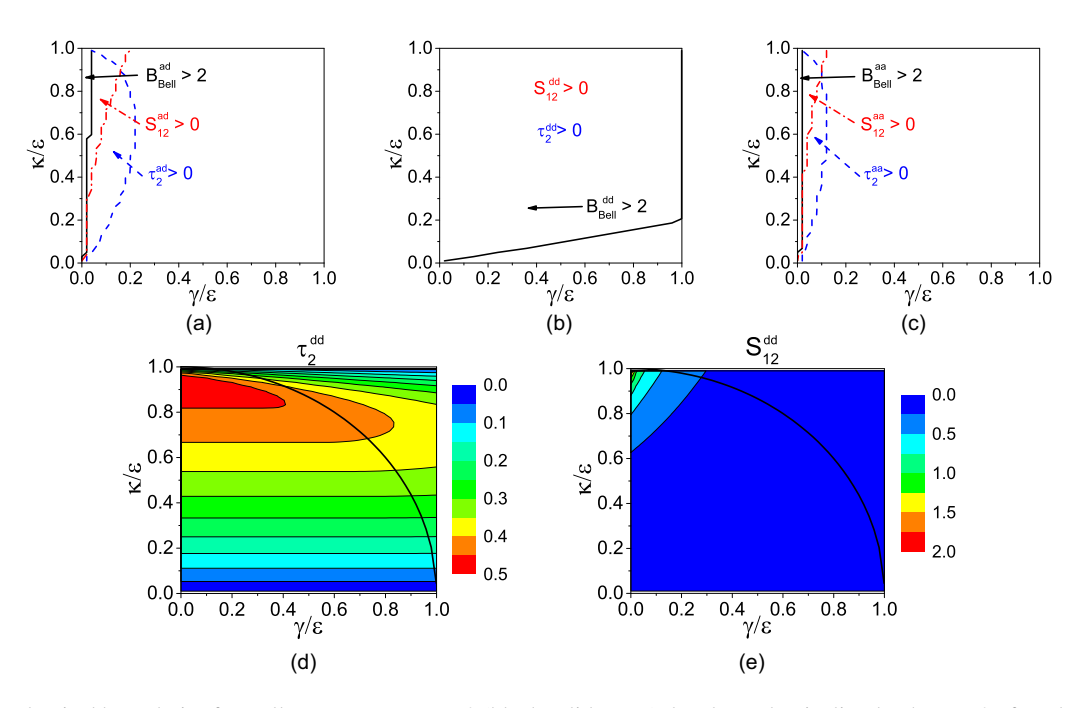


FIG. 7. Nonclassical boundaries for Bell parameter $B_{\text{Bell}} > 2$ (black solid curve), local nonclassicality depth $\tau_2 > 0$ of mode 2 (blue dashed curves), and steering parameter $S_{1 \to 2} > 0$ (red dashed-dotted curves) in the plane of model parameters γ/ϵ and κ/ϵ drawn for (a) standard, (b) passive, and (c) active PTSSs. In (b), $\tau_2 > 0$ and $S_{1 \to 2} > 0$ hold for all model parameters. (d) Local nonclassicality depth τ_2^{dd} of mode 2 and (e) steering parameter $S_{1 \to 2}^{\text{dd}}$ for passive PTSS are shown as they depend on model parameters γ/ϵ and κ/ϵ ; solid black curves identify positions of EPs in passive PTSS. The superscript notation is explained in Fig. 1.

discussed above, which are defined as the maxima taken over the dimensionless time ϵt .

Moreover, we find that states exhibiting the Bell nonlocality, as the states with the strongest nonclassicality, are effectively generated only in systems without amplification, across broad ranges of the system parameters [see Fig. 4]. For comparison, these ranges are plotted in Figs. 7(a), 7(b), and 7(c) for the standard, passive, and active PTSSs, respectively. Even weak amplification prevents the system from generating the Bell-nonlocal states. In contrast, steerable and entangled states are observed in standard, passive, and active PTSSs for any values of the system parameters. Steering is, however, strongly asymmetric. In the system with amplification, the nonamplified mode is steerable for any value of the system parameters, but the amplified mode is steerable only for very weak values of the considered damping or amplification [see Figs. 3(c) and 6(c); compare the boundaries in Figs. 7(a) to 7(c); see also Fig. 7(e)].

Similarly, the nonamplified mode exhibits local nonclassicality for any values of the system parameters. This is not the case for observing local nonclassicality in the amplified mode, which requires smaller values of the considered damping or amplification constants [see Figs. 2(d) and 5(d); compare the boundaries in Figs. 7(a) to 7(c); see also Fig. 7(d)].

In the case of the standard PTSS, the states violating the Bell inequalities, the states in which the amplified mode exhibits local nonclassicality, and the states allowing steering of the amplified mode cannot be generated across the entire range of system parameters. These states are reached only for small values of the damping and amplification constants. In contrast, entangled and steerable states are easily obtained throughout the full parameter space.

VIII. EVOLUTION OF THE NEGATIVITY, NONCLASSICALITY DEPTH, AND THEIR GENERATION SPEED

Above we compared the maximal values of nonclassicality depths and several quantifiers of quantum correlations attained during the system evolution. Here, we address the process of nonclassical-state generation in a more detailed way by analyzing the times needed to arrive at these maximal values and speeds of their generation in the standard PTSS. As typical examples, we investigate in Figs. 8(a) to 8(d) the times t and speeds v belonging to the negativity E_N and local nonclassicality depth τ_1 of mode 1. We can see in Figs. 8(a) to 8(d), (first row), that greater values of the damping and amplification constants γ shorten these times $t_{E_N}^{\text{ad}}$ and $t_{\tau_1}^{\text{ad}}$ and also slow down the negativity (speed $v_{E_N}^{\text{ad}}$) and nonclassicality (speed $v_{\tau_1}^{\rm ad}$) generation. Contrary to this, greater values of the nonlinear coupling constant κ/ϵ make the times $t_{E_N}^{\rm ad}$ and $t_{\tau_1}^{\rm ad}$ longer and the speed $v_{E_N}^{\rm ad}$ of negativity generation faster. However, the maximal speeds $v_{\tau_1}^{\rm ad}$ of mode-1 nonclassicality generation are reached for $\kappa/\epsilon \approx 0.6$. This is caused by the interplay of the increasing ability to generate nonclassical states and slowing down the system evolution when moving towards an EP with the increasing nonlinear constant κ/ϵ

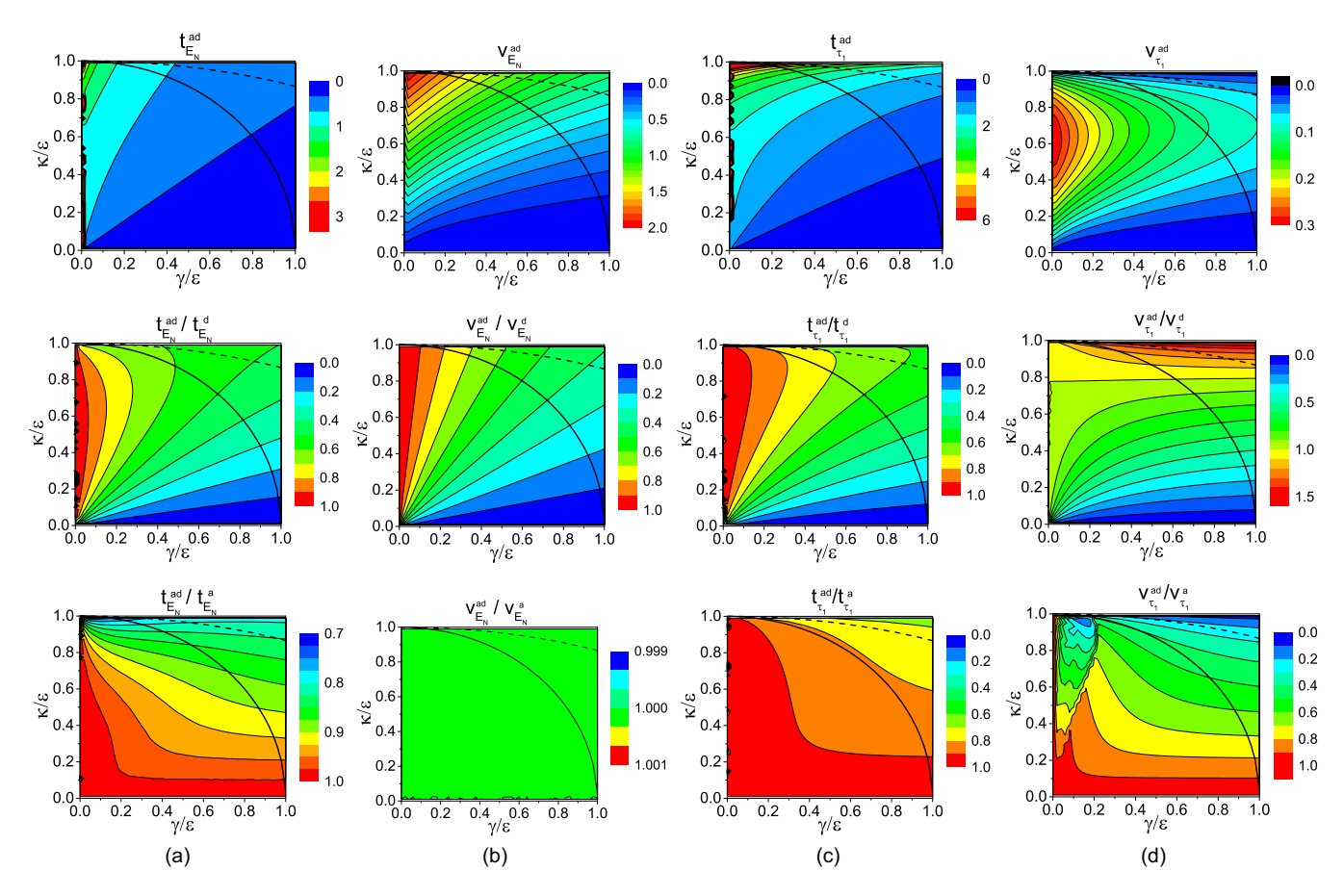


FIG. 8. (a) Time instant $t_{E_N}^{\rm ad}$ corresponding to the maximal negativity E_N , (b) maximal speed $v_{E_N}^{\rm ad}$ of the negativity generation, (c) time instant $t_{\tau_1}^{\rm ad}$ yielding the maximal nonclassicality depth τ_1 of mode 1, and (d) maximal speed $v_{\tau_1}^{\rm ad}$ of nonclassicality-depth τ_1 generation in standard PTSS as they depend on model parameters γ/ϵ and κ/ϵ . The values of the drawn parameters are compared with those originating in the model with considered only damping (superscript d) and only amplification (superscript d). Solid (dashed) black curves identify positions of EPs in PTSS (systems with only damping and only amplification). The superscript notation is explained in Fig. 1.

Comparing the behavior of the standard PTSS with the systems with only damping [see Figs. 8(a) to 8(d), (second row)] and only amplification [see Figs. 8(a) to 8(d), (third row)], the maximal values of negativity E_N and local nonclassicality τ_1 are always reached faster in the standard PTSS. The maximal speeds $v_{E_N}^{\mathrm{ad}}$ of negativity generation are always greater for the system with only damping which accords with greater maximal values of the negativity E_N reached in this system. Interestingly, the maximal speeds $v_{E_N}^{\rm ad}$ are very close in the standard PTSS and the system with only amplification, as documented in Fig. 8(b), (third row). The maximal speed $v_{\tau}^{\rm ad}$ of mode-1 nonclassicality generation in the standard PTSS is usually smaller than those of the systems with only damping and only amplification. Only when $\kappa/\epsilon \ge 0.8$, amplification in mode 2 of the standard system and the resulting larger amplitudes of the mode allows for faster mode-1 nonclassicality generation compared to the system with only damping Fig. 8(d), (second row).

The generally lower maximum values of nonclassicality depths and the analyzed quantum-correlation quantifiers observed in the standard PTSS, compared to systems with only damping or only amplification, can be attributed to two key factors: a shorter duration of nonclassical-state generation and a slower buildup of nonclassical properties. This qualitatively

resembles the behavior of fields in nonlinear three-mode parametric processes with phase mismatch [18].

The above findings, which identify the passive PTSS as the most efficient source of nonclassical states, support its practical implementation, especially since achieving damping is generally simpler than achieving amplification. The realization requires a nonlinear medium with a strong $\chi^{(2)}$ nonlinearity [18]. When such a medium is placed inside a resonator, the resonator enhances the effective nonlinearity and simultaneously introduces damping to both frequency down-converted modes through leakage via the resonator mirrors. Adding a birefringent material to the resonator, which linearly couples the modes, then completes the formation of a passive PTSS. It is worth noting that nonlinear $\chi^{(2)}$ crystals inside resonators have been reliable sources of squeezed light for decades [58,59].

We note that realizing an active PTSS is also feasible, for example, using spin-polarized laser technology. In these lasers, two optical modes coexist, each pumped by electrons polarized in orthogonal spin directions (left-to-right and right-to-left). The natural coupling between these modes in various photonic heterostructures enables the formation of an active PTSS [60]. In Refs. [61–63], such spin-polarized lasers featuring exceptional points were ana-

lyzed, with field saturation effectively acting as a Kerr-type nonlinearity.

IX. CONCLUSIONS

Numerical analysis of two bosonic modes coupled linearly and by parametric down-conversion performed across the full range of system parameters reveals that the standard \mathcal{PT} -symmetric system (PTSS), characterized by balanced damping and amplification, does not, in general, enhance the system's ability to generate nonclassical states of light. This conclusion is supported across the entire hierarchy of nonclassicality and quantum correlations by comparing in turn the nonclassicality depths, negativity, steering parameters, and the Bell parameter for the standard PTSSs and related systems affected solely by either damping or amplification.

While the standard PTSS outperforms its active counterpart, where one mode is undamped and the other is doubly amplified, it is clearly outperformed by the passive variant, in which one mode is doubly damped and the other is unaffected by amplification. This is particularly notable because all three systems possess identical eigenvectors and real parts of their eigenfrequencies. Their differing behavior arises from distinct characteristics of the fluctuating forces accompanying damping and amplification (involving spontaneous emission).

The reduced ability of the standard PTSS to generate nonclassical states can be attributed to two factors: a shorter time window over which nonclassical properties arise and a slower rate at which these properties develop. In conclusion, the most significant benefits of the PTSS dynamics in physically nonlinear systems are realized in the passive PTSSs configuration. Such systems can generate highly nonclassical states (featuring entanglement, quantum steering, and Bell nonlocality) across wide parameter ranges. They also allow for practical experimental realizations based on parametric down-conversion in crystals embedded into optical resonators.

ACKNOWLEDGMENTS

J.P. acknowledges support by Project No. 25-15775S of the Czech Science Foundation. K.B., G.C., A.K.-K., and A.M. were supported by the Polish National Science Centre (NCN) under the Maestro Grant No. DEC-2019/34/A/ST2/00081. J.K.K. and W.L. acknowledge the support provided by the program of the Polish Ministry of Science entitled "Regional Excellence Initiative," Project No. RID/SP/0050/2024/1. J.P. also acknowledges support by the Project No. ITI CZ.02.01.01/00/23_021/0008790 of the Ministry of Education, Youth, and Sports of the Czech Republic and EU.

DATA AVAILABILITY

Data for the graphs presented in the paper are available at [64].

- C. M. Bender and S. Boettcher, Real spectra in non-Hermitian Hamiltonians having PT symmetry, Phys. Rev. Lett. 80, 5243 (1998).
- [2] C. M. Bender, S. Boettcher, and P. N. Meisinger, PT-symmetric quantum mechanics, J. Math. Phys. 40, 2201 (1999).
- [3] C. M. Bender, D. C. Brody, and H. F. Jones, Must a Hamiltonian be Hermitian? Am. J. Phys. 71, 1095 (2003).
- [4] S. K. Özdemir, S. Rotter, F. Nori, and L. Yang, Parity-time symmetry and exceptional points in photonics, Nat. Mater. 18, 783 (2019).
- [5] M. Miri and A. Alù, Exceptional points in optics and photonics, Science **363**, eaar7709 (2019).
- [6] Z.-P. Liu, J. Zhang, S. K. Özdemir, B. Peng, H. Jing, X.-Y. Lü, C.-W. Li, L. Yang, F. Nori, and Y.-X. Liu, Metrology with PT-symmetric cavities: Enhanced sensitivity near the PT-phase transition, Phys. Rev. Lett. 117, 110802 (2016).
- [7] W. Chen, Ş. K. Özdemir, G. Zhao, J. Wiersig, and L. Yang, Exceptional points enhance sensing in an optical microcavity, Nature (London) 548, 192 (2017).
- [8] H. Hodaei, U. H. Absar, S. Wittek, H. Garcia-Gracia, R. El-Ganainy, D. N. Christodoulides, and M. Khajavikhan, Enhanced sensitivity at higher-order exceptional points, Nature (London) 548, 187 (2017).
- [9] B. He, S.-B. Yan, J. Wang, and M. Xiao, Quantum noise effects with Kerr-nonlinearity enhancement in coupled gain-loss waveguides, Phys. Rev. A 91, 053832 (2015).
- [10] S. Vashahri-Ghamsari, B. He, and M. Xiao, Continuous-variable entanglement generation using a hybrid \mathcal{PT} -symmetric system, Phys. Rev. A **96**, 033806 (2017).

- [11] J. Peřina, Jr. and A. Lukš, Quantum behavior of a \mathcal{PT} symmetric two-mode system with cross-Kerr nonlinearity,
 Symmetry 11, 1020 (2019).
- [12] J. Peřina, Jr., A. Lukš, J. K. Kalaga, W. Leoński, and A. Miranowicz, Nonclassical light at exceptional points of a quantum *PT*-symmetric two-mode system, Phys. Rev. A 100, 053820 (2019).
- [13] B. Peng, Ş. K. Özdemir, F. Lei, F. Monifi, M. Gianfreda, G. L. Long, S. Fan, F. Nori, C. Bender, and L. Yang, Parity–time-symmetric whispering-gallery microcavities, Nat. Phys. 10, 394 (2014).
- [14] L. Chang, X. Jiang, S. Hua, C. Yang, J. Wen, L. Jiang, G. Li, G. Wang, and M. Xiao, Parity-time symmetry and variable optical isolation in active-passive-coupled microresonators, Nat. Photon. 8, 524 (2014).
- [15] Z. Lin, H. Ramezani, T. Eichelkraut, T. Kottos, H. Cao, and D. N. Christodoulides, Unidirectional invisibility induced by PT-symmetric periodic structures, Phys. Rev. Lett. 106, 213901 (2011).
- [16] A. Regensburger, C. Bersch, M.-A. Miri, G. Onishchukov, D. N. Christodoulides, and U. Peschel, Parity-time synthetic photonic lattices, Nature (London) 488, 167 (2012).
- [17] S. Scheel and A. Szameit, \mathcal{PT} -symmetric photonic quantum systems with gain and loss do not exist, Europhys. Lett. 122, 34001 (2018).
- [18] R. W. Boyd, Nonlinear Optics (Academic, New York, 2003).
- [19] L. Mandel and E. Wolf, Optical Coherence and Quantum Optics (Cambridge University Press, Cambridge, England, 1995).

- [20] J. Peřina, Quantum Statistics of Linear and Nonlinear Optical Phenomena (Kluwer, Dordrecht, The Netherlands, 1991).
- [21] J. Peřina, Jr. and J. Peřina, Quantum statistics of nonlinear optical couplers, in *Progress in Optics*, edited by E. Wolf (Elsevier, Amsterdam, 2000), Vol. 41, pp. 361–419.
- [22] *Parity-Time Symmetry and its Applications*, edited by D. N. Christodoulides and J. Yang (Springer, Singapore, 2018).
- [23] C. M. Bender, *PT symmetry, in Quantum and Classical Physics* (World Scientific, Singapore, 2020).
- [24] V. V. Konotop, J. Yang, and D. A. Zezyulin, Nonlinear waves in PT-symmetric systems, Rev. Mod. Phys. 88, 035002 (2016).
- [25] L. Feng, R. El-Ganainy, and L. Ge, Non-Hermitian photonics based on parity-time symmetry, Nat. Photon. 11, 752 (2017).
- [26] S. K. Gupta, Y. Zou, X.-Y. Zhu, M.-H. Lu, L.-J. Zhang, X.-P. Liu, and Y.-F. Chen, Parity-time symmetry in non-Hermitian complex optical media, Adv. Mater. 32, 1903639 (2020).
- [27] R. El-Ganainy, K. G. Makris, M. Khajavikhan, Z. H. Musslimani, S. Rotter, and D. N. Christodoulides, Non-Hermitian physics and PT symmetry, Nat. Phys. 16, 15 (2020).
- [28] R. J. Glauber, Coherent and incoherent states of the radiation field, Phys. Rev. 131, 2766 (1963).
- [29] E. C. G. Sudarshan, Equivalence of semiclassical and quantum mechanical descriptions of statistical light beams, Phys. Rev. Lett. 10, 277 (1963).
- [30] J. Peřina, Jr., A. Miranowicz, J. K. Kalaga, and W. Leoński, Unavoidability of nonclassicality loss in *PT*-symmetric systems, Phys. Rev. A **108**, 033512 (2023).
- [31] G. Chimczak, A. Kowalewska-Kudlaszyk, E. Lange, K. Bartkiewicz, and J. Peřina, Jr., The effect of thermal photons on exceptional points in coupled resonators, Sci. Rep. 13, 5859 (2023).
- [32] J. Kadlec, K. Bartkiewicz, A. Černoch, K. Lemr, and A. Miranowicz, Experimental hierarchy of the nonclassicality of single-qubit states via potentials for entanglement, steering, and Bell nonlocality, Opt. Express 32, 2333 (2024).
- [33] C. T. Lee, Measure of the nonclassicality of nonclassical states, Phys. Rev. A 44, R2775 (1991).
- [34] S. A. Hill and W. K. Wootters, Computable entanglement, Phys. Rev. Lett. 78, 5022 (1997).
- [35] R. Horodecki, P. Horodecki, M. Horodecki, and K. Horodecki, Quantum entanglement, Rev. Mod. Phys. **81**, 865 (2009).
- [36] E. G. Cavalcanti, S. J. Jones, H. M. Wiseman, and M. D. Reid, Experimental criteria for steering and the Einstein-Podolsky-Rosen paradox, Phys. Rev. A 80, 032112 (2009).
- [37] J. S. Bell, On the Einstein-Podolsky-Rosen paradox, Phys. Phys. Fiz. 1, 195 (1964).
- [38] F. Minganti, A. Miranowicz, R. W. Chhajlany, and F. Nori, Quantum exceptional points of non-Hermitian Hamiltonians and Liouvillians: The effects of quantum jumps, Phys. Rev. A 100, 062131 (2019).
- [39] J. Peřina, Jr., A. Miranowicz, G. Chimczak, and A. Kowalewska-Kudlaszyk, Quantum Liouvillian exceptional and diabolical points for bosonic fields with quadratic Hamiltonians: The Heisenberg-Langevin equation approach, Quantum 6, 883 (2022).
- [40] K. Thapliyal, J. Peřina, Jr., A. K. G. Chimczak, and A. Miranowicz, Multiple quantum exceptional, diabolical, and hybrid points in multimode bosonic systems: I. Inherited and genuine singularities, arXiv:2405.01666.

- [41] J. Peřina, Jr., K. Thapliyal, A. K. G. Chimczak, and A. Miranowicz, Multiple quantum exceptional, diabolical, and hybrid points in multimode bosonic systems: II. Nonconventional pt-symmetric dynamics and unidirectional coupling, arXiv:2405.01667.
- [42] W. Vogel, D. G. Welsch, and S. Walentowicz, *Quantum Optics* (Wiley-VCH, Weinheim, Germany, 2001).
- [43] P. Meystre and M. Sargent III, *Elements of Quantum Optics* (Springer, Berlin, 2007).
- [44] S. B. Jaäger, T. Schmit, G. Morigi, M. J. Holland, and R. Betzholz, Lindblad master equations for quantum systems coupled to dissipative bosonic modes, Phys. Rev. Lett. 129, 063601 (2022).
- [45] G. Adesso and F. Illuminati, Entanglement in continuous variable systems: Recent advances and current perspectives, J. Phys. A: Math. Theor. 40, 7821 (2007).
- [46] H. Risken, The Fokker-Planck Equation: Methods of Solution and Applications (Springer, Berlin, 1989).
- [47] G. S. Agarwal and K. Qu, Spontaneous generation of photons in transmission of quantum fields in \mathcal{PT} -symmetric optical systems, Phys. Rev. A **85**, 031802(R) (2012).
- [48] V. Peřinová, A. Lukš, and J. Křepelka, Quantum description of a PT-symmetric nonlinear directional coupler, J. Opt. Soc. Am. B 36, 855 (2019).
- [49] P.-C. K. J.-D. Lin, N. Lambert, A. Miranowicz, F. Nori, and Y.-N. Chen, Non-Markovian quantum exceptional points, Nat. Commun. 16, 1289 (2025).
- [50] A. Peres, Separability criterion for density matrices, Phys. Rev. Lett. 77, 1413 (1996).
- [51] P. Horodecki, Separability criterion and inseparable mixed states with positive partial transposition, Phys. Lett. A 232, 333 (1997).
- [52] R. Simon, Peres-Horodecki separability criterion for continuous variable systems, Phys. Rev. Lett. 84, 2726 (2000).
- [53] K. Banaszek and K. Wódkiewicz, Nonlocality of the Einstein-Podolsky-Rosen state in the Wigner representation, Phys. Rev. A 58, 4345 (1998).
- [54] K. Banaszek and K. Wódkiewicz, Testing quantum nonlocality in phase space, Phys. Rev. Lett. 82, 2009 (1999).
- [55] S. Olivares and M. G. A. Paris, Enhancement of nonlocality in phase space, Phys. Rev. A 70, 032112 (2004).
- [56] K. Thapliyal and J. Peřina, Jr., Ideal pairing of the Stokes and anti-Stokes photons in the Raman process, Phys. Rev. A 103, 033708 (2021).
- [57] J. Kadlec, K. Bartkiewicz, A. Černoch, K. Lemr, and A. Miranowicz, Experimental relative entanglement potentials of single-photon states, Phys. Rev. A 110, 023720 (2024).
- [58] M. Mehmet, S. Ast, T. Eberle, S. Steinlechner, H. Vahlbruch, and R. Schnabel, Squeezed light at 1550 nm with a quantum noise reduction of 12.3 db, Opt. Express 19, 25763 (2011).
- [59] A. I. Lvovsky and M. G. Raymer, Continuous-variable optical quantum state tomography, Rev. Mod. Phys. 81, 299 (2009).
- [60] M. Drong, T. Fordos, H. Y. Jaffres, J. Peřina, Jr., K. Postava, J. Pištora, and H. J. Drouhin, Local and mean-field approaches for modeling semiconductor spin-lasers, J. Opt. 22, 055001 (2020).
- [61] M. Drong, T. Fordos, H. Y. Jaffres, J. Peřina, Jr., K. Postava, P. Ciompa, J. Pištora, and H. J. Drouhin, Spin-VCSELs with local optical anisotropies: Toward terahertz polarization modulation, Phys. Rev. Appl. 15, 014041 (2021).

- [62] M. Drong, M. Dems, J. Peřina, Jr., T. Fordos, H. Y. Jaffres, K. Postava, and H. J. Drouhin, Time-dependent laser cavity perturbation theory: Exploring future nano-structured photonic devices in semi-analytic way, J. Lightwave Technol. 40, 4735 (2022).
- [63] M. Drong, J. Peřina Jr., T. Fördös, H. Y. Jaffrès, K. Postava, and H.-J. Drouhin, Spin vertical-cavity surface-emitting lasers with linear gain anisotropy: Prediction of exceptional points
- and nontrivial dynamical regimes, Phys. Rev. A 107, 033509 (2023).
- [64] J. Perina, K. Bartkiewicz, G. Chimczak, A. Kowalewska-Kudaszyk, A. Miranowicz, J. Kalaga, and W. Leonski, Quantumness and its hierarchies in PT-symmetric down-conversion models [Data set], In Physical Review A (1.0), Zenodo (2025), https://doi.org/10.5281/zenodo.17243232.